Accepted Manuscript

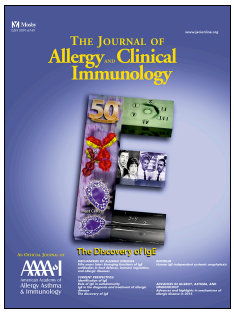

Type I IFN related NETosis in Ataxia Telangiectasia and Artemis deficiency

Ersin Gul, MSc, Esra Hazar Sayar, MD, Bilgi Gungor, PhD, Fehime Kara Eroglu, MD, Naz Surucu, MSc, Sevgi Keles, MD, Sukru Nail Guner, MD, Sıddıka Fındık, MD, Esin Alpdündar, MSc, Ihsan Cihan Ayanoglu, MSc, Basak Kayaoglu, MSc, Busra Nur Geçkin, BSc, Hatice Asena Sanli, BSc, Tamer Kahraman, PhD, Cengiz Yakicier, MD, Meltem Muftuoglu, PhD, Berna Oguz, MD, Deniz Nazire Cagdas Ayvaz, MD/PhD, Ihsan Gursel, PhD, Seza Ozen, MD, Ismail Reisli, MD, Mayda Gursel, PhD

PII: S0091-6749(17)31762-1

DOI: 10.1016/j.jaci.2017.10.030

Reference: YMAI 13125

To appear in: *Journal of Allergy and Clinical Immunology*

Received Date: 13 May 2017

Revised Date: 30 September 2017

Accepted Date: 18 October 2017

Please cite this article as: Gul E, Sayar EH, Gungor B, Eroglu FK, Surucu N, Keles S, Guner SN, Fındık S, Alpdündar E, Ayanoglu IC, Kayaoglu B, Geçkin BN, Sanli HA, Kahraman T, Yakicier C, Muftuoglu M, Oguz B, Cagdas Ayvaz DN, Gursel I, Ozen S, Reisli I, Gursel M, Type I IFN related NETosis in Ataxia Telangiectasia and Artemis deficiency, *Journal of Allergy and Clinical Immunology* (2017), doi: 10.1016/j.jaci.2017.10.030.

Impaired DNA damage repair in AT and Artemis deficient patient cells promote cytosolic DNA-mediated type I IFN production, priming neutrophils to undergo NETosis.

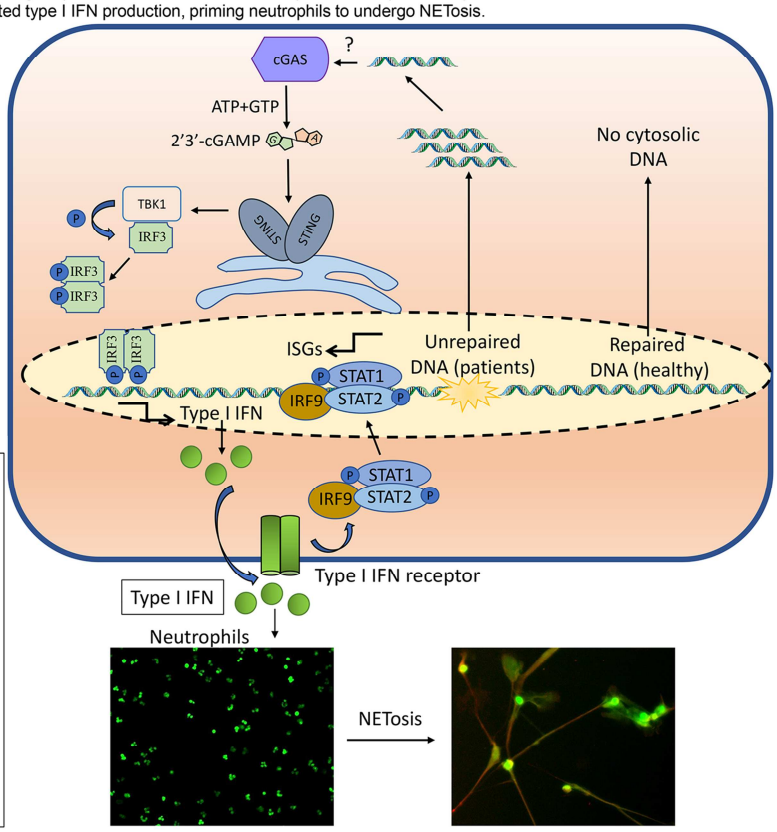

Abbreviations	
cGAS	Cyclic GMP-AMP synthase
cGAMP	cyclic GMP-AMP
STING	Stimulator of interferon genes
TBK1	TANK Binding Kinase 1
IRF	Interferon regulatory factor
STAT	Signal transducer and activator of transcription
ISGs	Interferon stimulated genes
IFN	Interferon
NETosis	generation of Neutrophil Extracellular Traps

Type I IFN related NETosis in Ataxia Telangiectasia and Artemis deficiency

Ersin Gul, MSc[a*], Esra Hazar Sayar, MD[b*], Bilgi Gungor, PhD[a*], Fehime Kara Eroglu, MD[c], Naz Surucu, MSc[a], Sevgi Keles, MD[b], Sukru Nail Guner, MD[b], Sıddıka Fındık, MD[d], Esin Alpdündar, MSc[a], Ihsan Cihan Ayanoglu, MSc[a], Basak Kayaoglu, MSc[a], Busra Nur Geçkin, BSc[a], Hatice Asena Sanli, BSc[a], Tamer Kahraman, PhD[c], Cengiz Yakicier, MD[e], Meltem Muftuoglu, PhD[e], Berna Oguz, MD[f], Deniz Nazire Cagdas Ayvaz, MD/PhD[g], Ihsan Gursel, PhD[c], Seza Ozen, MD[h], Ismail Reisli, MD[b], Mayda Gursel, PhD[a]

[a]Department of Biological Sciences, Middle East Technical University, Ankara, Turkey

[b]Department of Immunology and Allergy, Meram Medical Faculty, Necmettin Erbakan University, Konya, Turkey

[c]Thorlab, Therapeutic Oligodeoxynucleotide Research Laboratory,' Department of Molecular Biology and Genetics, Ihsan Dogramaci Bilkent University, Ankara, Turkey

[d]Department of Pathology, Meram Medical Faculty, Necmettin Erbakan University, Konya, Turkey

[e]Department of Molecular Biology and Genetics, Acibadem Mehmet Ali Aydinlar University

[f]Department of Radiology, Hacettepe University Medical Faculty, Ankara, Turkey

[g]Department of Pediatric Immunology, Hacettepe University Medical Faculty, Ankara, Turkey

[h]Department of Pediatric Rheumatology, Hacettepe University Medical Faculty, Ankara, Turkey

[*]**These 3 authors contributed equally to this work**

Co-corresponding Authors:

1. Mayda Gursel (for experimental section and manuscript correspondence)

Address: Middle East Technical University, Department of Biological Sciences, 06800, Ankara, Turkey, e-mail: mgursel@metu.edu.tr

2. Ismail Reisli and Seza Ozen (for clinical data on AT/Artemis deficient and SAVI patients, respectively)

Abstract

Background

Pathological inflammatory syndromes of unknown etiology are commonly observed in Ataxia telangiectasia (AT) and Artemis deficiency. Similar inflammatory manifestations also exist in STING-associated vasculopathy in infancy (SAVI) patients.

Objective

To test the hypothesis that the inflammation associated manifestations observed in AT and Artemis deficient patients stem from increased type I IFN signature leading to neutrophil mediated pathological damage.

Methods

Cytokine/protein signatures were determined by ELISA, cytometric bead array or by qPCR. Stat1 phosphorylation levels were determined by flow cytometry. DNA species accumulating in the cytosol of patients' cells was quantified microscopically and flow cytometrically. Propensity of isolated polymorhonuclear granulocytes to form neutrophil extracellular traps (NETs) was determined using fluorescence microscopy and picogreen assay. Neutrophil reactive oxygen species levels and mitochondrial stress were assayed using fluorogenic probes, microscopy and flow cytometry.

Results

Type-I and III interferon signatures were elevated in plasma and peripheral blood cells of AT, Artemis deficient and SAVI patients. Chronic interferon production stemmed from accumulation of DNA in cytoplasm of AT and Artemis deficient cells. Neutrophils isolated from patients spontaneously produced neutrophil extracellular traps (NETs) and displayed indicators of oxidative and mitochondrial stress, supportive of their NETotic

tendencies. A similar phenomenon was also observed in neutrophils from healthy controls exposed to patient plasma samples or exogeneous IFNα.

Conclusion

Type I IFN-mediated neutrophil activation and NET formation may contribute to inflammatory manifestations observed in AT, Artemis deficient and SAVI patients. Thus, neutrophils represent a promising target to manage inflammatory syndromes in diseases with active type I IFN signature.

Key messages

Impaired DNA damage repair in AT and Artemis deficient patient cells promote accumulation of DNA species in cytosol, provoking type I IFN production.

Neutrophils isolated from patients spontaneously produced neutrophil extracellular traps (NETs) and displayed indicators of oxidative and mitochondrial stress.

Neutrophils represent a promising target to manage inflammatory syndromes in diseases with active type I IFN signature.

Keywords

Primary immunodeficiencies; Autoinflammation; Ataxia Telangiectasia; Artemis deficiency; Type I Interferon; Interferonopathy; Neutrophil extracellular traps; NETosis

79

80

81 **Capsule summary**

82 Enhanced type I IFN response observed in AT, Artemis deficiency and SAVI, exert
83 tissue damage through neutrophil-driven chronic processes, providing a common target
84 to manage inflammatory syndromes in diseases with active type I IFN signature.

85

List of Abbreviations

AT	Ataxia Telangiectasia
ATM	Ataxia telangiectasia mutated
SCID	Severe combined immunodeficiency
SAVI	STING-associated vasculopathy with onset in infancy
NET	neutrophil extracellular trap
SLE	Systemic lupus erythematosus
IP-10	Interferon-inducible protein 10
ISGs	Interferon stimulated genes
PBMC	peripheral blood mononuclear cells
MPO	myeloperoxidase
LDGs	Low density granulocytes
ROS	Reactive oxygen species

Introduction

Constitutive type I interferon production in the absence of infection can be detrimental to the host, promoting severe inflammation. In this context, an increasing number of heterogeneous diseases with elevated IFN signatures are being classified under the spectrum of “type I interferonopathies” (1-4). Dysregulation in nucleic acid removal or recognition is thought to contribute to accumulation of endogenous nucleic acid ligands or constitutive activation of nucleic acid sensing signaling pathways, culminating in excessive type I interferon production. Accumulating evidence also suggests a link between DNA damage repair mechanisms and type I interferon production. Elevated IFN stimulated gene signatures were observed in cells exposed to DNA-damage (5-9). Of note, DNA damage was demonstrated to stimulate leakage of genome-derived DNA species into the cytosol, thereby inducing the expression of type I interferons (10). Interestingly, in Ataxia Telangiectasia (AT) patients with loss of function mutations in the DNA repair protein ataxia telangiectasia mutated (ATM), unrepaired DNA lesions led to release and accumulation of single stranded DNA species into the cytosol, inducing type I IFNs via a cGAS/STING-dependent mechanism (11). AT is a complex inherited multisystem disease characterized by progressive neurodegeneration, combined immunodeficiency, radiosensitivity and a predisposition to malignancy (12). Pathological inflammatory and autoimmune syndromes of unknown etiology have been reported in many AT patients (11,13-18). Mutations in the DCLRE1C gene encoding Artemis, another DNA double strand break repair protein further involved in V(D)J recombination during T- and B- cell development (19-20), cause immunodeficiency phenotypes ranging from radiosensitive severe combined immunodeficiency (SCID) to mere antibody deficiency, with frequent autoimmune and inflammatory manifestations (21-26). It is possible that similar to AT, unrepaired DNA fragments can leak into the cytosol in Artemis deficient cells and initiate type I IFN production, promoting chronic inflammation. To test this hypothesis, we compared the immune status of AT and Artemis deficient patients to healthy controls and to a patient with a recently identified severe interferonopathy, SAVI (STING-associated vasculopathy with onset in infancy), caused by a gain-of-function mutation in the TMEM173 gene encoding the adaptor signaling protein STING (27). This syndrome is

characterized by neonatal-onset systemic inflammation with cutaneous vasculopathy, skin lesions and interstitial lung disease.

Similar to some AT and SAVI patients, unexplained inflammatory skin lesions, erythematous papules and lung injury (bronchiectasis) are observed in Artemis deficient patients (14,23,28-29), suggestive of a common underlying immune dysregulation in pathogenesis of these diseases. In this context, neutrophil extracellular trap (NET) formation and neutrophil-related tissue injury has been linked to the pathophysiology of a broad spectrum of diseases, including systemic lupus erythematosus (SLE) (30-34), wherein enhanced NET formation was associated with interferon alpha signaling (35). Therefore, a possible role of NETs in the chronic inflammatory responses observed in AT, Artemis deficient and SAVI patients was also investigated.

Methods

Participants

Samples from a suspected SAVI patient and his parents were submitted for study after written informed consent had been obtained. The protocol was approved by the institutional review board of Hacettepe University Medical Faculty, Ankara. To detect TMEM173 gene mutations, exons (3 to 8) were amplified, followed by bidirectional Sanger sequencing (see the Methods section in the Supplementary Appendix). The patient was confirmed to have a de novo N154S mutation in exon V, consistent with a previously defined SAVI phenotype (27).

Samples from the AT and Artemis deficient patients and healthy donors were submitted for study after written informed consent had been obtained. All Artemis deficient patients had hypomorphic Artemis mutations (homozygous missense mutation c.194C>T in DCLRE1C gene) with minimal residual recombination efficiency, and were of age between 5 to 21 years. AT patients were either diagnosed clinically or carried various mutations as reported in Supplementary Table 1. Age of AT patients ranged from 4 to 17. Healthy donor age ranged from 5 to 22. The protocol was approved by the institutional review board of Necmettin Erbakan University Medical Faculty, Konya.

Cytokine measurements and functional studies

Circulating and PBMC-secreted or expressed cytokine/chemokine/protein levels and gene expression analyses were performed according to cytometric bead array, ELISA or qRT-PCR based standard procedures and are described in the Supplementary Methods. IP-10 and phosphorylated Stat1 levels whithin PBMCs were determined by intracellular cytokine/protein staining and flow cytometry. Cytosolic ssDNA or dsDNA levels in healthy and patient PBMCs were determined microscopically or flow cytometrically in untreated or UV treated permeabilized cells stained for single stranded or double stranded DNA specific antibodies. Healthy or patient neutrophils were analyzed for Neutrophil Extracellular Trap (NET) formation using fluorescence microscopy of samples stained for total DNA, extracellular DNA and/or myeloperoxidase. Amount of NETs released was quantified using a micrococcal nuclease digestion/picogreen quantitation based spectrofluorometric assay. Cytosolic and mitochondrial reactive oxygen species levels in neutrophils were assessed flow cytometrically using ROS reactive probes Dihydrorhodamine 123 and MitoSox Red, respectively. Neutrophil associated mitochondrial stress response was assessed using microscopic imaging or flow cytometric analysis of mitochondrial membrane potential sensitive JC-1 dye stained neutrophils. Details of the methods employed are provided in the Supplementary Methods section.

Results

Autoimmune/autoinflammatory manifestations in AT, Artemis Deficient and SAVI patients in relation to elevated type I interferon activity

Ataxia Telangiectasia (AT), Artemis deficient and SAVI patients frequently suffer from severe autoimmune/autoinflammatory complications. Skin lesions with neutrophilic infiltrates and interstitial lung disease are commonly observed in Artemis deficient patients and in SAVI (Fig. 1a). In the case of SAVI, the observed inflammation and immunopathology was linked to excessive type I IFN production (27). However, factor(s) instigating chronic inflammation in AT and Artemis deficient individuals remain poorly

understood. Recent evidence suggests that unrepaired DNA double strand breaks stimulate type I IFN production in AT patients which may account for the observed chronic inflammatory manifestations (11). Whether spontaneous type I interferon production is also an underlying mechanism contributing to chronic inflammation in Artemis deficient patients, remained unexplored.

To test the hypothesis that the inflammation associated manifestations observed in AT and Artemis deficient patients may result from an increased type I IFN signature, we compared the immune status of AT and Artemis deficient patients to healthy controls and to a patient with SAVI carrying the N154S (c.461A>G) mutation in exon V of TMEM173 gene (as a positive control of a known type I interferonopathy; Supplementary Fig. S1). All Artemis deficient patients harbored identical hypomorphic mutations in exon 3 of DCLRE1C gene encoding the protein Artemis (c.194C>T; p.T65I) as previously reported (23,24). Ataxia Telangiectasia patients included in this study received a clinical diagnosis and in 5 patients, the mutation was determined (Supplementary Table S1). Clinical characteristics, hematological and serological findings of all patients enrolled in this study are summarized in Supplementary Tables S1, S2 and S3, respectively.

We observed that the plasma levels of interferon-alpha (multiple subtypes), interferon-inducible protein 10 (IP-10) and interferon λ1 (IL-29) were significantly elevated in all patient groups (Fig.1b and Supplementary Fig.S2). There was no increase in circulating levels of other pro-inflammatory cytokines tested (IL-8, IL-17, IL-1β, TNFα and IL-6; supplementary Fig.S2). Furthermore, peripheral blood mononuclear cells (PBMC) from patients spontaneously secreted IFNα2a and IP-10 into culture supernatants in the absence of any stimulation (Fig. 1c and Supplementary Fig.S3). When stimulated with the STING ligand 2'3'-cGAMP, AT and Artemis deficient patient cells produced higher levels of IFNα2a and IP-10 than healthy controls (Supplementary Fig.S4), whereas as expected, the SAVI patient's elevated responses could not be stimulated further with cGAMP (27). Consistent with the elevated type I IFN associated cytokine/chemokine levels, unstimulated patient cells had significantly higher levels of phosphorylated STAT1 (pSTAT1) than healthy controls (Fig. 1d). Stat1 is an important

transcription factor that is phosphorylated in response to type-I interferon signaling and controls the induction of interferon stimulated genes (ISGs). Therefore, we also assessed the expression of two ISGs in PBMC samples by qRT-PCR and found that the transcription of MX1 (Fig.1e) and ISG15 (Supplementary Fig. S5) was upregulated in patient samples.

These results are of interest since they not only confirm the existence of exaggerated type I interferon signaling in AT patients but demonstrate a similar phenomenon in Artemis deficient patients for the first time. Furthermore, our results also suggest that these 2 diseases could be classified as “interferonopathies” and could share certain clinical features with SAVI patients.

DNA spontaneously accumulates in the cytosol of AT and Artemis deficient patient cells

DNA damage can incite accumulation of cytoplasmic DNA species, thereby activating cytosolic DNA sensing pathways (5-11). We therefore assessed cytosolic levels of ssDNA or dsDNA species in healthy and patient PBMCs that were either untreated or exposed to UV-induced DNA damage. The extent of spontaneous DNA leakage was consistently higher in untreated patient cells than healthy controls (Fig. 2a and 2b, left panels). UV-induced DNA damage stimulated cytosolic DNA release in healthy cells and exaggerated the leakage response in patient cells (Fig. 2b, right panels). Of interest, the staining protocols were first established in THP-1 and TREX-1 deficient THP-1 cells to exclude the possibility that the antibodies would breach the nuclear membrane and interact with nuclear material (supplementary Figure S6).

To evaluate whether the detected cytosolic DNA was of nuclear and/or mitochondrial origin, cytosolic extracts from 2 AT and 2 Artemis deficient patients were

prepared. Samples were assessed for the absence of mitochondrial and nuclear contamination using the mitochondrial and nuclear markers VDAC and Lamin A/C, respectively, in comparison to a whole cell extract, nuclear extract and mitochondrial extract prepared from HCT 116 cell line as a positive control of each fraction (Fig. 2c). Cytosolic extracts were then analyzed for nuclear and mitochondrial DNA by qPCR (Fig. 2d). Results demonstrated that patient cytosolic extracts contained DNA of both mitochondrial (103 bp ND5 mitochondrial DNA) and nuclear (133 bp H3 nuclear DNA) origin. Our data suggest that impaired DNA damage repair in AT and Artemis deficient patient cells promote accumulation of DNA species in cytosol, provoking type I IFN induced sterile inflammation.

AT, Artemis deficient and SAVI patient neutrophils spontaneously produce NETs

Increased interferon signature is consistently demonstrated in peripheral blood of SLE patients (36). Furthermore, neutrophils isolated from SLE patients exhibit abnormal features such as increased aggregation and a tendency to undergo spontaneous NETosis, suggestive of a link between elevated levels of type I interferons and neutrophil-mediated disease pathogenesis (37). In fact, one preliminary study has shown that blocking of IFNα signaling in neutrophils reduced neutrophil extracellular trap formation in murine lupus (35). To date, except for SLE, neutrophil functions in diseases strongly associated with increased type I interferon signature (like SAVI) have never been tested. Therefore, to assess whether spontaneously activated neutrophils contribute to pathological damage in AT, Artemis deficiency and SAVI, we isolated patient neutrophils and compared their propensity to form NETs with respect to cells obtained from healthy donors.

Blood polymorphonuclear granulocytes of AT, Artemis deficient and SAVI patients spontaneously released NETs (Fig.3a and Supplementary Fig.S7) visualized as red stained extracellular DNA (using cell impermeable dye SYTOX Orange over

Hoechst stained total DNA (blue)). The amount of DNA associated with NETs was also quantified spectrofluorometrically using a micrococcal nuclease/picogreen-based assay. Healthy neutrophils released very low amounts of DNA, while AT, Artemis deficient and SAVI patient cells released ~5-, 4- and 2.5-fold more NET-associated DNA, respectively (Fig.3b). The extruded nuclear material was also associated with the neutrophil granular protein myeloperoxidase (MPO), indicative of its NETotic origin (Fig. 3c). To further validate the activation status of neutrophils in blood, we next determined the concentration of neutrophil elastase in patient vs healthy plasmas. Results showed that AT, Artemis deficient and SAVI patients had significantly higher levels of elastase in their plasma compared to healthy controls (Fig. 3d), suggestive of neutrophil over-activation. Percent of a distinct subset of low density, pathogenic granulocytes is frequently elevated in blood of patients with autoimmune/autoinflammatory manifestations (38). We found that in 4 of the 6 AT and Artemis deficient patients tested, the percentage of low-density granulocytes (LDGs) was substantially increased (compared to healthy controls, average LDG % was 8- and 7-fold higher in AT and Artemis deficient patients, respectively, although this increase was not significant in the AT group; Supplementary Fig. S8), suggesting that pathogenic LDGs could also contribute to chronic inflammation in these patients.

AT, Artemis deficient and SAVI patient plasma samples and recombinant IFNα trigger NET release from healthy neutrophils

Next, to determine whether patient plasma-associated factor(s) contributed to NET formation, neutrophils from healthy donors were cultured in the presence of healthy or patient plasma samples. Results revealed that patient but not healthy plasma samples stimulated healthy neutrophils to undergo NETosis and release their DNA as NETs (Fig.4a and supplementary Fig.S9). Furthermore, patient-plasma induced NETosis was inhibited in healthy PMNs pretreated with the JAK inhibitor Tofacitinib (supplementary Fig.S10), suggesting that elevated type-I interferon related cytokines/chemokines may contribute to NET formation in healthy neutrophils. To

validate this assumption, healthy neutrophils were treated with either recombinant interferon alpha or recIFNγ. Neutrophils exposed to recIFNα but not to recIFNγ extruded significantly higher levels of DNA than untreated controls (Fig. 4b) and the extracellular filaments of chromatin were associated with MPO (Fig. 4c), suggestive of NETotic death.

Type I IFNs mediate oxidative and mitochondrial stress in neutrophils

Reactive oxygen species (ROS) production has been reported as an integral part of a variety of NETosis triggering stimuli (39). In AT, chronic oxidative stress and mitochondrial damage have been implicated as factors underlying disease pathogenesis (40). We therefore examined the intracellular levels of ROS in patient cells using the cytosolic and mitochondrial ROS indicators Dihydrorhodamine 123 (DHR123) and MitosoxRed, respectively. Freshly isolated neutrophils from AT and Artemis deficient patients displayed 2-fold more DHR123 fluorescence than healthy controls (Fig.5a), indicative of ongoing chronic oxidative stress. Of note, in this experiment, two of the 6 Artemis deficient patients had recently undergone bone marrow transplantation 6 months earlier (shown as purple lines in histogram plots in Fig. 5a). Although such small sample size and post-transplantation duration is inappropriate to derive definitive conclusions, preliminary evidence suggests that oxidative stress is not alleviated following hematopoietic stem cell transplantation. Analysis of mitochondrial superoxide anion levels using MitosoxRed revealed no significant differences between patient cells and healthy controls (Supplementary Fig.S11). However, AT and Artemis deficient patient neutrophils exposed to recIFNα produced 2-fold more mitochondrial superoxide anion than healthy neutrophils incubated with identical dose of the cytokine (Fig. 5b), suggesting that type I IFNs can exacerbate mitochondrial ROS production and therefore may contribute to mitochondrial damage. To test this hypothesis, JC-1 stained neutrophils from 3 different subjects were incubated without or with recIFNα for 30 minutes, and mitochondrial health was

determined using microscopic images and flow cytometric analysis of cells positive for red JC-1 aggregates (healthy mitochondria) versus green JC-1 monomers (damaged, hypopolarized mitochondria). Healthy neutrophils not exposed to recIFNα had lower levels of depolarized mitochondria (Fig. 5c). However, within 30 minutes of incubation with recIFNα, monomeric green JC-1 dye fluorescence intensity was enhanced in ~30-40 % of cells, suggesting that type I IFNs induce mitochondrial ROS (Fig. 5b) and cause mitochondrial membrane depolarization. To examine whether the observed spontaneous ROS (Fig. 5a) and type I IFN-induced exaggerated mitochondrial ROS (Fig. 5b) in patient neutrophils correlated with mitochondrial dysfunction, freshly isolated patient neutrophils were stained with JC-1 and analyzed without exposure to any cytokines. Five of the 6 AT patients and all of the 6 Artemis deficient patient neutrophils, including the 2 that had received bone marrow transplantation, exhibited higher percentages of JC-1 green positive neutrophils (Fig. 5d) when compared to healthy controls (Fig. 5c, untreated healthy neutrophils). These results indicate that the ongoing chronic oxidative stress in patient neutrophils and extended exposure to type I IFNs may alter mitochondrial functions in neutrophils and facilitate neutrophil extracellular trap formation.

Our data suggests that type I IFNs contribute to NETosis. Although spontaneous NETosis observed in patient neutrophils may in part depend on elevated type I IFNs, a lack of DNA repair and accumulated DNA damage could potentially represent cell-intrinsic factors exacerbating NETosis. To adress this question, healthy neutrophils were left untreated or treated with H_2O_2 alone (DNA damage inducing agent), KU-55933 alone (ATM inhibitor) or a combination of H_2O_2 and KU-55933. Absence or presence of NETs were evaluated at the end of 5 h of incubation using fluorescence microscopy and the picogreen assays (Fig. 6a and 6b, respectively). Data indicated that DNA damage alone (400 µM H_2O_2) had no measurable effect on healthy neutrophils. However, the highest dose of ATM inhibitor alone and all doses of the combined inhibitor and H_2O_2 triggered NET formation, suggesting that DNA damage in the absence of repair can

initiate NETosis. Collectively, our data advocate for a role of both type I IFNs and DNA damage defect underlying the NETotic phenotype of patient cells.

Discussion

Herein, we showed that AT and Artemis deficiencies share certain features with known interferonopathies as evidenced by high levels of circulating type I and III IFNs, spontaneous secretion of IFNα and intracellular production of IP-10 in patient cells, increased pSTAT1 levels and elevated expression of ISGs in PBMCs. Our data suggest that in the case of AT and Artemis deficiency, this enhanced type I IFN response most likely stems from defective DNA repair-associated cytosolic DNA accumulation in patient cells, triggering type-I interferon secretion through the cGAS-STING cytosolic nucleic acid sensing pathway.

SAVI and several other autoinflammatory/autoimmune diseases display a unique signature of type I interferon activity, suggesting a common underlying mechanism of clinical pathologies, including systemic inflammation, skin lesions, and pulmonary disease (1-4,27). The pathogenic mechanism(s) behind the type I IFN-inflicted tissue damage is unclear. Published work on SLE patients and ADA2 deficient individuals (a monogenic type I-interferonopathy) indicate that neutrophil mediated mechanisms, and in particular NETs, might be involved in this damage response (30-34, 41). Whether or not neutrophils contribute to autoinflammatory/autoimmune phenomena in Artemis deficient patients (vitiligo, Hashimoto's thyroiditis, juvenile idiopatic arthritis and granulomatous skin lesions (23)) and SAVI, remained unexplored. In case of AT, patient neutrophils were shown to overproduce pro-inflammatory cytokines but whether they formed pathological NETs was not investigated (13). Herein, we showed that unlike healthy neutrophils, AT, Artemis deficient and SAVI patient neutrophils spontaneously released their DNA in the form of NETs. Furthermore, we established that incubation with patient plasma samples or recIFNα was sufficient to stimulate NETosis in healthy neutrophils. Exposure to recombinant IFNα primed neutrophils to produce ROS, an important prerequisite of NETosis. Consistent with the chronic type I interferon signature in AT and Artemis deficient cells, unprimed patient neutrophils displayed indicators of oxidative and mitochondrial stress responses. Collectively, these results indicate that

394 the enhanced type I IFN response observed in AT, Artemis deficiency and SAVI, might
395 exert tissue damage through neutrophil-driven chronic processes.

396 Infection-independent NET formation has been implicated in the pathophysiology
397 of several diseases, including thrombosis (42–46), autoimmune diseases (44, 47–52),
398 inflammation (37, 53–56), type I diabetes (57, 58), pulmonary diseases (59–63) and
399 fibrosis (64). NETotic DNA released from neutrophils is in an oxidized state which acts
400 on plasmacytoid dendritic cells (pDCs) to potently stimulate more type I IFN production
401 through a TLR9-dependent process (30,37). Since our data suggests that IFNα primes
402 neutrophils to produce ROS and release NET DNA, it is plausible that the released NET
403 DNA might promote further type I IFN production from pDCs, completing a viscous
404 positive feedback cycle of chronic interferon production (Fig. 7). Furthermore, our
405 results also indicate that DNA damage in the absence of repair can initiate NETosis,
406 implying that both type I IFNs and DNA damage defect underlies the NETotic phenotype
407 of patient cells. Our study was restricted to Artemis deficient patients with hypomorphic
408 mutations in which the mutant protein displayed residual nuclease activity, enabling
409 limited V(D)J recombination and hence a “leaky” SCID phenotype. Although this
410 presents as a milder immunodeficiency when compared to patients with DCLRE1C
411 loss-of-function alleles and typical SCID phenotype, susceptibility to develop
412 autoimmunity/autoinflammation is also higher (24). Therefore, whether a similar
413 NETotic neutrophil phenotype also exists in Artemis deficient patients with loss of
414 function mutations remains to be determined.

415 In summary, our results implicate that neutrophil activation and particularly NET
416 formation may inflict tissue damage in seemingly unrelated diseases with elevated type
417 I IFN signatures. In this context, we propose that drugs that can interfere with ROS
418 production, neutrophil activation and/or NETosis and therapies blocking interferon
419 signaling could ameliorate organ damage and might be of benefit in the management of
420 sterile inflammatory manifestations of AT, Artemis deficiency and SAVI. In conclusion,
421 we showed that patients with AT and hypomorphic Artemis mutations have similar
422 characteristics with well-defined interferonopathies, and high levels of type I IFNs may

contribute to inflammatory manifestations in such diseases via IFN-mediated neutrophil activation and NET formation.

Figure Legends

Figure 1. Autoimmune/autoinflammatory features in patients and identifiers of elevated type I IFN signatures.

Panel **a** shows the autoinflammatory skin manifestations and evidence of interstitial lung disease in Artemis deficient and SAVI patients. Vascular inflammation with neutrophilic infiltrates are observed in skin lesion biopsy samples (Hematoxylin and eosin, original magnification ×400 (Artemis sample) and x40 (SAVI sample). Panel **b** shows increased levels of circulating IFNα and IP-10 in AT (n=10), Artemis deficient (n=10) and SAVI (n=1; 2 separate measurements 1 month apart) patients as compared to healthy subjects (n=10). Panel **c** shows PBMCs from AT (n=10 and n=10), Artemis deficient (n=10 and n=8) and SAVI patients (n=1; 2 separate measurements 1 month apart) spontaneously secrete IFNα and intracellularly accumulate more IP-10, respectively than healthy control cells (n=9 and n=7). Panel **d** demonstrates that pSTAT1 levels in PBMCs of healthy subjects (blue) is significantly lower than those observed in AT (orange), Artemis deficient (red), SAVI (green) patients (flow cytometric histograms). MFI values obtained from histograms were also plotted and shown. Panel **e** shows increased expression of interferon-regulated gene MX1 in patients with AT (n=8) and Artemis deficiency (n=9), as compared with healthy controls (n=10) and to a patient with SAVI (n=1; 2 separate measurements 1 month apart). Data are representative of at least three independent experiments.

Figure 2. Increased levels of cytosolic ssDNA and dsDNA species in AT and Artemis deficient patients. Panel **a** depicts immunofluoresence microscopic analysis of cytosolic ssDNA (red) in Healthy, AT and Artemis deficient patient PBMCs. Nuclei were stained with Hoechst (blue). Each panel represents images from different individuals (n=3). Panel **b** shows flow cytometric analysis of untreated or UV treated cells from healthy (blue), AT (orange) or Artemis deficient (red) patients. Histograms in

each plot represent a different individual. Samples stained with isotype control (upper panels), anti-dsDNA (middle) and anti-ssDNA (bottom) are shown. Mean fluorescence intensities are reported in each panel. Panel **c** shows the absence of mitochondrial or nuclear contamination in cytosolic extracts prepared from patient cells. Whole cell extract (WCE), nuclear extract (NE) and mitochondrial extract (Mit E) prepared from a control cell line (HCT 116) was included as a positive control of each fraction. Panel **d** shows the 103 bp ND5 mitochondrial DNA (left gel image) and the 133 bp H3 nuclear DNA (right gel image) and cycle threshold (Ct) values for ND5 and H3 genes amplified by qPCR (Ct value graph) from cytosolic extracts. The boxes represent mean Ct values and the bars shows standard deviations from two independent experiments. Control indicates negative control in qPCR reaction without cytosolic DNA.

Figure 3. Analysis of spontaneous Neutrophil Extracellular Trap formation in patient neutrophils. Panels **a** and **c** show that patient neutrophils spontaneously produce NETs that are visible in samples stained with Sytox Orange (extracellular DNA), Hoechst (total DNA) and neutrophil myeloperoxidase (Panel **c**). PMA stimulated neutrophils served as positive control of NET formation (bottom images). Panel **b** shows the quantitation of released NET DNA from patient cells. All patient neutrophils (n=10 for AT and Artemis deficient and one SAVI) released significantly higher levels of DNA into culture supernatants than healthy control cells (n=10). Panel **d** depicts that patient plasma samples contained elevated levels of neutrophil activation marker elastase. Data is representative or combined from at least four independent experiments.

Figure 4. Analysis of patient plasma or recombinant IFNα-induced neutrophil extracellular trap formation in healthy neutrophils. Panels **a** and **b** shows that patient plasma samples and recIFNα trigger NET formation in healthy neutrophils, whereas healthy plasma or recIFNγ has no effect. Panel **c** shows that healthy neutrophils incubated with various doses of recIFNα release NETs that stain positive for DNA (blue) and myeloperoxidase (red). Plasma samples from different donors were tested on neutrophils from a single healthy donor. Data are representative of three independent experiments.

Figure 5. Analysis of cytosolic and mitochondrial ROS levels and measurement of mitochondrial stress in neutrophils. Panels **a** and **b** show that cytosolic (**a**) and mitochondrial (**b**) ROS levels are significantly elevated in unstimulated (**a**) or recIFNα stimulated (**b**) AT (n=6) and Artemis deficient (n=6) patient neutrophils as opposed to healthy controls (n=3). Both flow cytometric individual histograms and plotted MFI values are given. Two of the Artemis deficient patients that have received bone marrow transplantation are shown in purple. Panel **c** shows that unstimulated neutrophils isolated from healthy individuals (n=3) show low levels of monomeric JC-1 staining (green fluorescence in microscopy images and flow cytometry plots) that is upregulated following exposure to recIFNα, indicating mitochondrial membrane depolarization and stress. Panel **d** shows that unstimulated patient neutrophils displayed JC-1 monomer staining, indicative of ongoing stress response.

Figure 6. DNA damage in the absence of DNA repair triggers of Neutrophil Extracellular Trap formation in healthy neutrophils. Panel **a** shows that healthy neutrophils spontaneously produce NETs when exposed to the highest dose of ATM inhibitor (KU-55933; 250 µM) alone or all doses of the combined inhibitor and H_2O_2 (DNA damage inducing agent, 400 µM). NETs are visible in samples stained with Sytox Orange (extracellular DNA) and Syto Green (total DNA). Panel **b** shows the quantitation of released NET DNA from treated cells. Results are the average response of two healthy donor neutrophils ± SD.

Figure 7. Model of type I IFN-mediated chronic inflammation in AT, Artemis deficient and SAVI patients. In ATM and Artemis deficient cells, unrepaired DNA fragments leak into the cytosol, activating the nucleic acid sensing pathways (most probably the cGAS/cGAMP/STING pathway), stimulating TBK1-IRF3-dependent type I IFN production. In cells expressing a gain of function mutation in STING (SAVI patient), STING pathway is already active, independent of cytosolic DNA and/or 2'3'-cGAMP, resulting in constitutive type I IFN production. Type I IFNs act on cells expressing the type I IFN receptor, stimulating Stat1 and 2 protein phosphorylation dependent ISG expression. Ongoing oxidative stress in AT and Artemis deficient patient neutrophils and type I IFN-mediated mitochondrial ROS production and stress, primes neutrophils to

undergo NETosis. NET associated DNA may further contribute to type I IFN interferon secretion via plasmacytoid dendritic cells, exacerbating the inflammation.

Acknowledgements

We thank all the patients and their families who participated in this study. We also thank Mesut Muyan (Middle East Technical University, Department of Biological Sciences) for critical reading of the manuscript. This project was partially supported by TUBITAK grants 315S125, 115S430.

Competing Financial Interests

The authors declare no competing financial interests.

References

1. Crow YJ, Manel N. Aicardi-Goutières syndrome and the type I interferonopathies. Nat Rev Immunol 2015; 15:429-440.

2. Lee-Kirsch MA, Wolf C, Kretschmer S, Roers A. Type I interferonopathies-an expanding disease spectrum of immunodysregulation. Semin Immunopathol 2015; 37: 349-357.

3. de Jesus AA, Canna SW, Liu Y, Goldbach-Mansky R. Molecular mechanisms in genetically defined autoinflammatory diseases: disorders of amplified danger signaling. Annu Rev Immunol 2015, 33:823-874.

4. Rodero MP, Crow YJ. Type I interferon-mediated monogenic autoinflammation: The type I interferonopathies, a conceptual overview. J Exp Med 2016; 213:2527-2538.

5. Weichselbaum RR, Ishwaran H, Yoon T, Nuyten DS, Baker SW, Khodarev N, et al. An interferon-related gene signature for DNA damage resistance is a predictive marker for chemotherapy and radiation for breast cancer. Proc Natl Acad Sci USA 2008,105: 18490–18495.

6. Moschella F, Torelli GF, Valentini M, Urbani F, Buccione C, Petrucci, MT, et al. Cyclophosphamide induces a type I interferon-associated sterile inflammatory response

signature in cancer patients' blood cells: implications for cancer chemoimmunotherapy. Clin Cancer Res 2013; 19:4249–4261.

7. Yu Q, Katlinskaya YV, Carbone CJ, Zhao B, Katlinski KV, Zheng H, et al. DNA-damage-induced type I interferon promotes senescence and inhibits stem cell function. Cell Rep 2015; 11:785-797.

8. Brzostek-Racine S, Gordon C, Van Scoy S, Reich NC. The DNA damage response induces IFN. J Immunol 2011; 187:5336–5345.

9. Lam AR, Bert NL, Ho SS, Shen YJ, Tang LF, Xiong GM, et al. RAE1 ligands for the NKG2D receptor are regulated by STING-dependent DNA sensor pathways in lymphoma. Cancer Res 2014, 74:2193-2203.

10. Shen YJ, Le Bert N, Chitre AA, Koo CX, Nga XH, Ho SS, et al. Genome-derived cytosolic DNA mediates type I interferon-dependent rejection of B cell lymphoma cells. Cell Rep 2015, 11:460-473.

11. Härtlova A, Erttmann SF, Raffi FA, Schmalz AM, Resch U, Anugula S, et al. DNA damage primes the type I interferon system via the cytosolic DNA sensor STING to promote anti-microbial innate immunity. Immunity 2015; 42:332-343.

12. Lavin MF, Shiloh Y. The genetic defect in ataxia telangiectasia. Annu Rev Immunol 1997; 15:177-202.

13. Harbort CJ, Soeiro-Pereira PV, von Bernuth H, Kaindl AM, Costa-Carvalho BT, Condino-Neto A, et al. Neutrophil oxidative burst activates ATM to regulate cytokine production and apoptosis. Blood 2015; 126:2842-2851.

14. Drolet BA, Drolet B, Zvulunov A, Jacobsen R, Troy J, Esterly NB. Cutaneous granulomas as a presenting sign in ataxia-telangiectasia. Dermatology 1997;194:273-275.

15. Chiam LY, Verhagen MM, Haraldsson A, Wulffraat N, Driessen GJ, Netea MG, et al. Cutaneous granulomas in ataxia telangiectasia and other primary immunodeficiencies: reflection of inappropriate immune regulation? Dermatology 2011; 223:13-19.

16. Ammann AJ, Hong R. Autoimmune phenomena in ataxia telangiectasia. J Pediatr 1971; 78:821–826.

17. Kutukculer N, Aksu G. Is there an association between autoimmune hemolytic anemia and ataxia-telangiectasia? Autoimmunity 2000; 32:145–147.

18. McGrath-Morrow SA, Collaco JM, Crawford TO, Carson KA, Lefton-Greif MA, Zeitlin P, et al. Elevated serum IL-8 levels in ataxia telangiectasia. The Journal of Pediatrics 2010; 156:682–684.

19. Woodbine L, Brunton H, Goodarzi AA, Shibata A, Jeggo PA. Endogenously induced DNA double strand breaks arise in heterochromatic DNA regions and require ataxia telangiectasia mutated and Artemis for their repair. Nucl Acids Res 2011; 39:6986-6997.

20. Le Deist F, Poinsignon C, Moshous D, Fischer A, de Villartay J.P. Artemis sheds new light on V(D)J recombination. Immunol Rev 2004; 200:142–155.

21. Nowak-Wegrzyn A, Crawford TO, Winkelstein JA, Carson KA, Lederman HM. Immunodeficiency and infections in ataxia-telangiectasia. J Pediatr 2004; 144:505–511.

22. Schroeder SA, Zielen S. Infections of the respiratory system in patients with ataxia-telangiectasia. Pediatr Pulmonol 2013; 49:389–399.

23. Volk T, Pannicke U, Reisli I, Bulashevska A, Ritter J, Björkman A, et al. DCLRE1C (ARTEMIS) mutations causing phenotypes ranging from atypical severe combined immunodeficiency to mere antibody deficiency. Hum Mol Genet 2015; 24:7361-7372.

24. Felgentreff K, Lee YN, Frugoni F, Du L, van der Burg M, Giliani S, et al. Functional analysis of naturally occurring DCLRE1C mutations and correlation with the clinical phenotype of ARTEMIS deficiency. J Allergy Clin Immunol 2015; 136:140-150.

25. Lee PP, Woodbine L, Gilmour KC, Bibi S, Cale CM, Amrolia PJ, et al. The many faces of Artemis-deficient combined immunodeficiency - Two patients with DCLRE1C mutations and a systematic literature review of genotype-phenotype correlation. Clin Immunol 2013; 149:464-474.

26. Moshous D, Pannetier C, Chasseval Rd Rd, Deist Fl Fl, Cavazzana-Calvo M, Romana S, et al. Partial T and B lymphocyte immunodeficiency and predisposition to lymphoma in patients with hypomorphic mutations in Artemis. J Clin Invest 2003; 111:381-387.

27. Liu Y, Jesus AA, Marrero B, Yang D, Ramsey SE, Sanchez GAM, et al. Activated STING in a vascular and pulmonary syndrome N Engl J Med 2014; 371:507–518.

28. Ijspeert H, Lankester AC, van den Berg JM, Wiegant W, van Zelm MC, Weemaes CM, et al. Artemis splice defects cause atypical SCID and can be restored in vitro by an antisense oligonucleotide. Genes Immun 2011; 12:434-444.

29. Ege M, Ma Y, Manfras B, Kalwak K, Lu H, Lieber MR, et al. Omenn syndrome due to ARTEMIS mutations. Blood 2005; 105:4179-4186.

30. Garcia-Romo GS, Caielli S, Vega B, Connolly J, Allantaz F, Xu Z, et al. Netting neutrophils are major inducers of type I IFN production in pediatric systemic lupus erythematosus. Sci Transl Med 2011; 3:73ra20.

31. Villanueva E, Yalavarthi S, Berthier CC, Hodgin JB, Khandpur R, Lin AM, et al. Netting neutrophils induce endothelial damage, infiltrate tissues, and expose immunostimulatory molecules in systemic lupus erythematosus. J Immunol 2011; 187:538-552.

613 32. Denny MF, Yalavarthi S, Zhao W, Thacker SG, Anderson M, Sandy AR, et al. A
614 distinct subset of proinflammatory neutrophils isolated from patients with systemic lupus
615 erythematosus induces vascular damage and synthesizes type I IFNs. J Immunol 2010;
616 184:3284-3297.

617 33. Carmona-Rivera C, Zhao W, Yalavarthi S, Kaplan MJ. Neutrophil extracellular traps
618 induce endothelial dysfunction in systemic lupus erythematosus through the activation
619 of matrix metalloproteinase-2. Ann Rheum Dis 2015; 74:1417-1424.

620 34. Smith CK, Kaplan MJ. The role of neutrophils in the pathogenesis of systemic lupus
621 erythematosus. Curr Opin Rheumatol 2015, 27:448-453.

622 35. Furumoto Y, Smith CK, Blanco L, Zhao W, Brooks SR, Thacker SG, et al. Tofacitinib
623 ameliorates murine lupus and its associated vascular dysfunction. Arthritis Rheumatol
624 2017; 69:148-160.

625 36. Crow MK. Advances in understanding the role of type I interferons in systemic lupus
626 erythematosus. Curr Opin Rheumatol 2014; 26:467-474.

627 37. Lood C, Blanco LP, Purmalek MM, Carmona-Rivera C, De Ravin SS, Smith CK, et
628 al. Neutrophil extracellular traps enriched in oxidized mitochondrial DNA are
629 interferogenic and contribute to lupus-like disease. Nat Med 2016; 22:146-153.

630 38. Carmona-Rivera C, Kaplan MJ. Low-density granulocytes: a distinct class of
631 neutrophils in systemic autoimmunity. Semin Immunopathol 2013; 35:455-463.

632 39. Brinkmann V, Reichard U, Goosmann C, Fauler B, Uhlemann Y, Weiss DS, et al.
633 Neutrophil extracellular traps kill bacteria. Science 2004; 303:1532–1535.

634 40. Maciejczyk M, Mikoluc B, Pietrucha B, Heropolitanska-Pliszka E, Pac M, Motkowski
635 R, et al. Oxidative stress, mitochondrial abnormalities and antioxidant defense in Ataxia-
636 telangiectasia, Bloom syndrome and Nijmegen breakage syndrome. Redox Biol 2016;
637 11:375-383.

638 41. Belot A, Wassmer E, Twilt M, Lega JC, Zeef LA, Oojageer A, et al. Mutations in
639 CECR1 associated with a neutrophil signature in peripheral blood. Pediatr Rheumatol
640 Online J 2014; 12:44.

641 42. Kambas K, Mitroulis I, Apostolidou E, Girod A, Chrysanthopoulou A, Pneumatikos I,
642 et al. Autophagy mediates the delivery of thrombogenic tissue factor to neutrophil
643 extracellular traps in human sepsis. PLoS One 2012; 7:e45427.

644 43. Kambas K, Mitroulis I, Ritis K. The emerging role of neutrophils in thrombosis-the
645 journey of TF through NETs. Front Immunol 2012; 3:385.

646 44. Kambas K, Chrysanthopoulou A, Vassilopoulos D, Apostolidou E, Skendros P,
647 Girod A, et al. Tissue factor expression in neutrophil extracellular traps and neutrophil
648 derived microparticles in antineutrophil cytoplasmic antibody associated vasculitis may

promote thromboinflammation and the thrombophilic state associated with the disease. Ann Rheum Dis 2014; 73:1854–1863.

45. de Boer OJ, Li X, Teeling P. Neutrophils, neutrophil extracellular traps and interleukin-17 associate with the organisation of thrombi in acute myocardial infarction. Thromb Haemost 2013; 109:290–297.

46. Stakos DA, Kambas K, Konstantinidis T, Mitroulis I, Apostolidou E, Arelaki S, et al. Expression of functional tissue factor by neutrophil extracellular traps in culprit artery of acute myocardial infarction. Eur Heart J 2015; 36:1405–1414.

47. Hakkim A, Fürnrohr BG, Amann K, Laube B, Abed UA, Brinkmann V, et al. Impairment of neutrophil extracellular trap degradation is associated with lupus nephritis. Proc Natl Acad Sci USA 2010; 107:9813–9818.

48. Lande R, Ganguly D, Facchinetti V, Frasca L, Conrad C, Gregorio J, et al. Neutrophils activate plasmacytoid dendritic cells by releasing self-DNA-peptide complexes in systemic lupus erythematosus. Sci Transl Med 2011; 3:73ra19.

49. Kahlenberg JM, Kaplan MJ. Little peptide, big effects: the role of LL-37 in inflammation and autoimmune disease. J Immunol 2013; 191:4895–4901.

50. Leffler J, Martin M, Gullstrand B, Tydén H, Lood C, Truedsson L, et al. Neutrophil extracellular traps that are not degraded in systemic lupus erythematosus activate complement exacerbating the disease. J Immunol 2012; 188:3522–3531.

51. Couser WG, Johnson RJ. What is myeloperoxidase doing in ANCA-associated glomerulonephritis? Kidney Int 2015; 88:938–940.

52. Söderberg D, Kurz T, Motamedi A, Hellmark T, Eriksson P, Segelmark M. Increased levels of neutrophil extracellular trap remnants in the circulation of patients with small vessel vasculitis, but an inverse correlation to anti-neutrophil cytoplasmic antibodies during remission. Rheumatology (Oxford) 2015; 54:2085–2094.

53. Apostolidou E, Skendros P, Kambas K, Mitroulis I, Konstantinidis T, Chrysanthopoulou A, et al. Neutrophil extracellular traps regulate IL-1β-mediated inflammation in familial Mediterranean fever. Ann Rheum Dis 2016; 75:269–277.

54. Mitroulis I, Kambas K, Chrysanthopoulou A, Skendros P, Apostolidou E, Kourtzelis I, et al. Neutrophil extracellular trap formation is associated with IL-1β and autophagy-related signaling in gout. PLoS One 2011; 6:e29318.

55. Bennike TB, Carlsen TG, Ellingsen T, Bonderup OK, Glerup H, Bøgsted M, et al. Neutrophil extracellular traps in ulcerative colitis: a proteome analysis of intestinal biopsies. Inflamm Bowel Dis 2015; 21:2052–2067.

56. He Z, Si Y, Jiang T, Ma R, Zhang Y, Cao M, et al. Phosphotidylserine exposure and neutrophil extracellular traps enhance procoagulant activity in patients with inflammatory bowel disease. Thromb Haemost 2016; 115:738–751.

686 57. Menegazzo L, Ciciliot S, Poncina N, Mazzucato M, Persano M, Bonora B, et al.
687 NETosis is induced by high glucose and associated with type 2 diabetes. Acta Diabetol
688 2015; 52:497–503.

689 58. Wang Y, Xiao Y, Zhong L, Ye D, Zhang J, Tu Y, et al. Increased neutrophil elastase
690 and proteinase 3 and augmented NETosis are closely associated with β-cell
691 autoimmunity in patients with type 1 diabetes. Diabetes 2014; 63:4239–4248.

692 59. Cheng OZ, Palaniyar N. NET balancing: a problem in inflammatory lung diseases.
693 Front Immunol 2013:4.

694 60. Grabcanovic-Musija F, Obermayer A, Stoiber W, Krautgartner WD, Steinbacher P,
695 Winterberg N, et al. Neutrophil extracellular trap (NET) formation characterises stable
696 and exacerbated COPD and correlates with airflow limitation. Respir Res 2015; 16:59.

697 61. Marcos V, Zhou-Suckow Z, Önder Yildirim A, Bohla A, Hector A, Vitkov L, et al. Free
698 DNA in cystic fibrosis airway fluids correlates with airflow obstruction. Mediators
699 Inflamm 2015; 2015:408935.

700 62. Dwyer M, Shan Q, D'Ortona S, Maurer R, Mitchell R, Olesen H, et al. Cystic fibrosis
701 sputum DNA has NETosis characteristics and neutrophil extracellular trap release is
702 regulated by macrophage migration-inhibitory factor. J Innate Immun 2014; 6:765–779.

703 63. Chrysanthopoulou A, Mitroulis I, Apostolidou E, Arelaki S, Mikroulis D,
704 Konstantinidis T, et al. Neutrophil extracellular traps promote differentiation and function
705 of fibroblasts. J Pathol 2014; 233:294–307.

706 64. Demers M, Krause DS, Schatzberg D, Martinod K, Voorhees JR, Fuchs TA, et al.
707 Cancers predispose neutrophils to release extracellular DNA traps that contribute to
708 cancer-associated thrombosis. Proc Natl Acad Sci USA 2012; 109:13076–13081.

709 65. Aaman MD, Sorensen MM, Hvitby C, Berquist BR, Muftuoglu M, Tian J, et al.
710 Cockayne syndrome group B protein promotes mitochondrial DNA stability by
711 supporting the DNA repair association with the mitochondrial membrane. FASEB J
712 2010; 24:2334-2346.

713

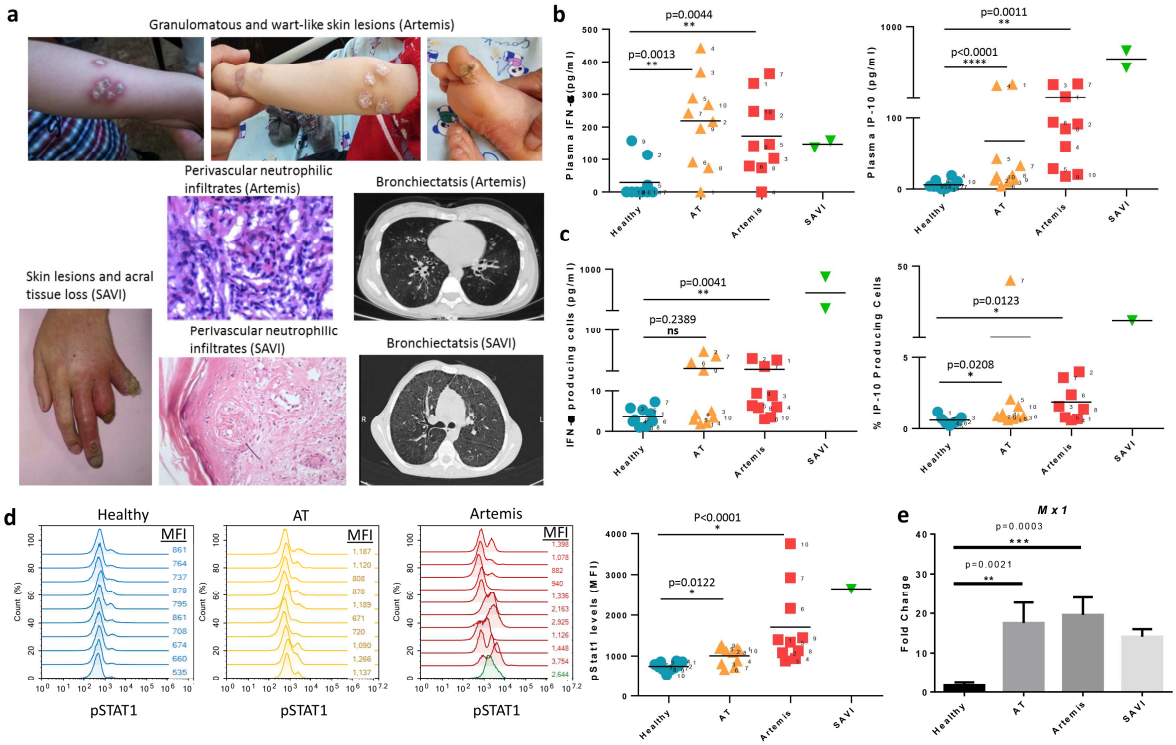

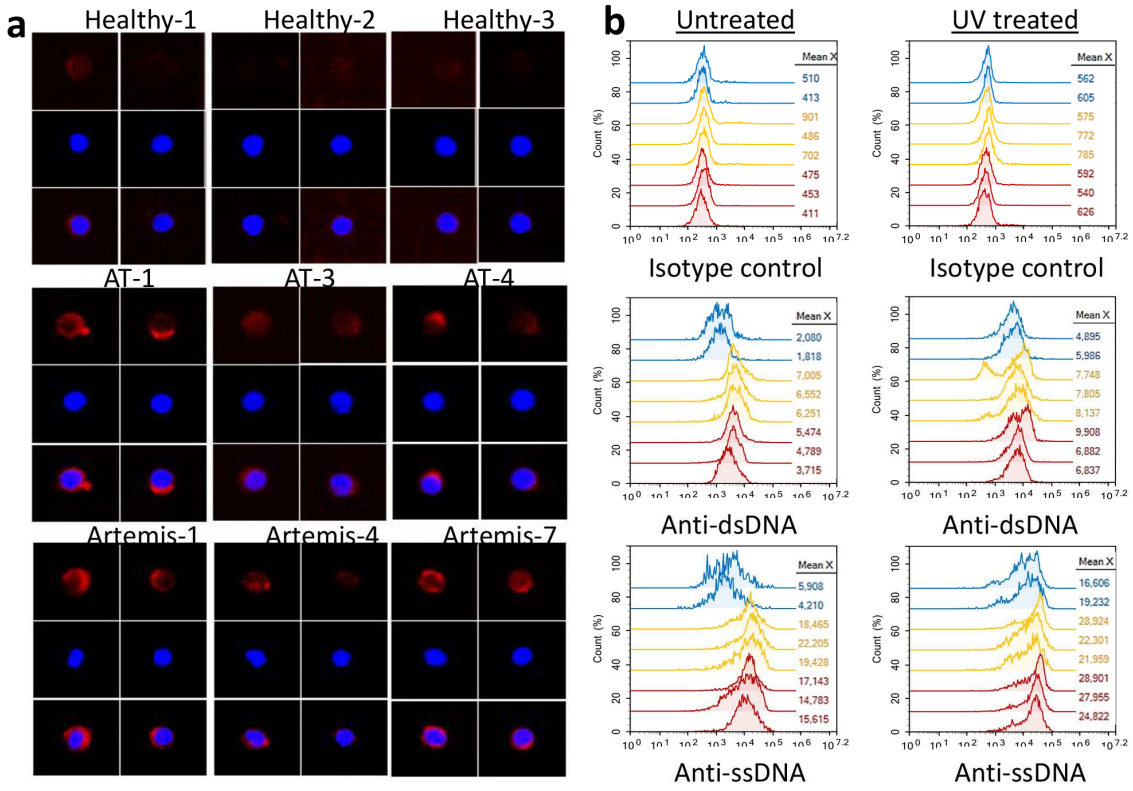
a
Healthy-1
Healthy-2
Healthy-3
AT-1
AT-3
AT-4
Artemis-1
Artemis-4
Artemis-7
b
Untreated
UV treated
Isotype control
Anti-dsDNA
Anti-ssDNA
Mean X
Count (%)

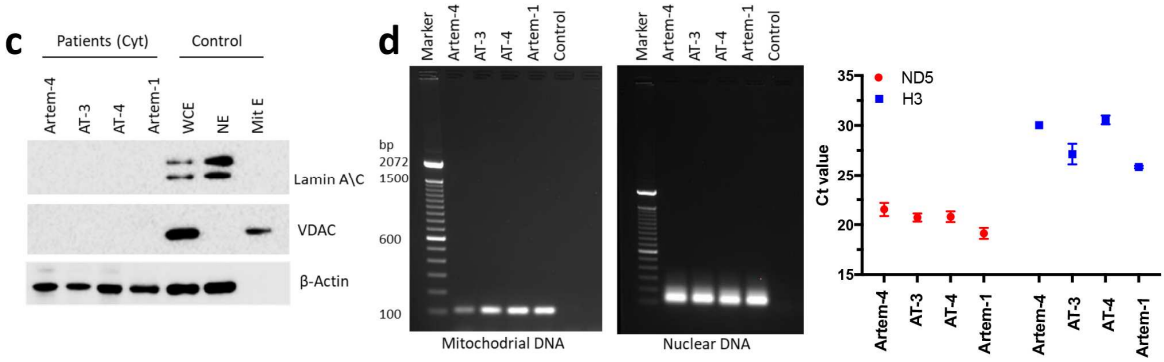
c
Patients (Cyt)
Control
Artem-4
AT-3
AT-4
Artem-1
WCE
NE
Mit E
Lamin A\C
VDAC
β-Actin
d
Marker
Artem-4
AT-3
AT-4
Artem-1
Control
bp
2072
1500
600
100
Mitochodrial DNA
Nuclear DNA
ND5
H3
Ct value

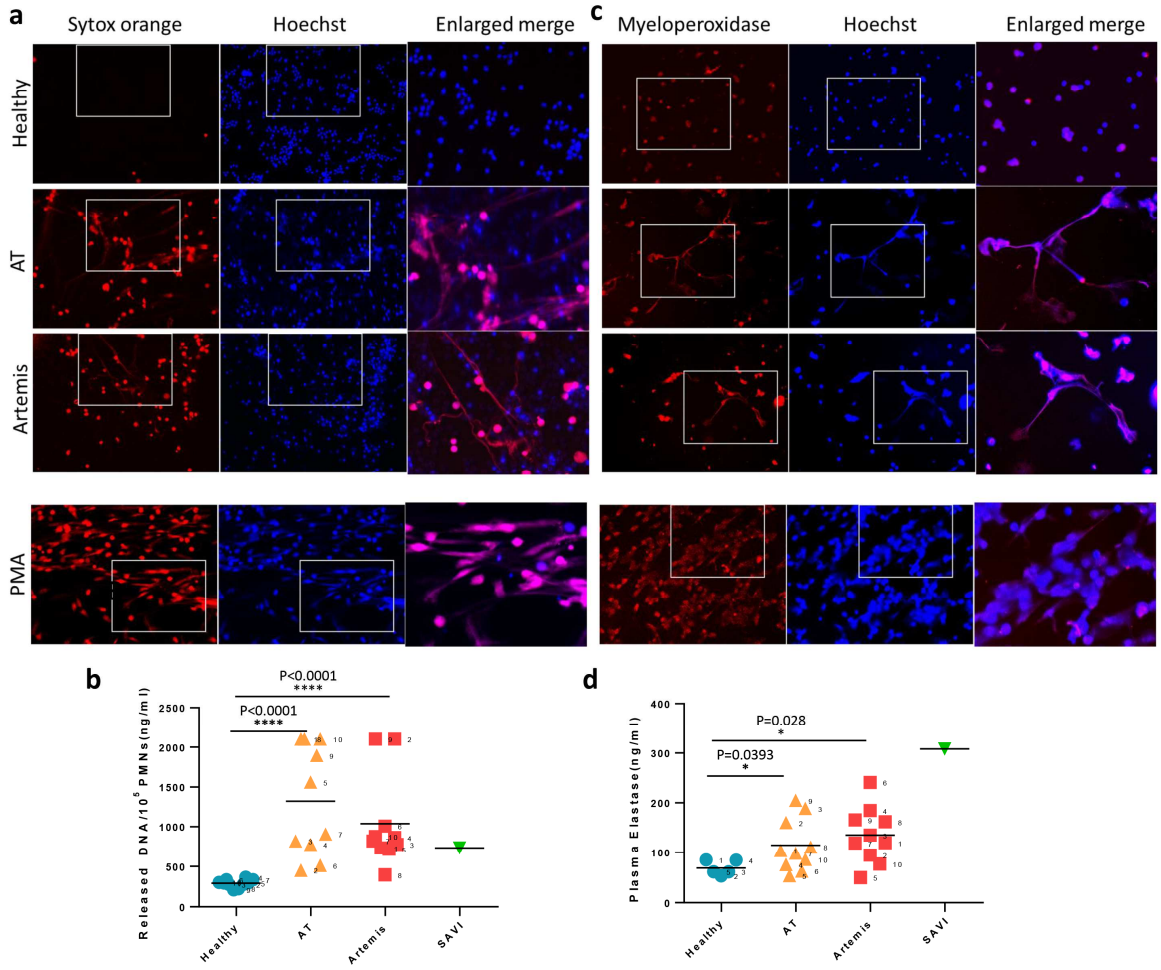
a
Sytox orange
Hoechst
Enlarged merge
Healthy
AT
Artemis
PMA
c
Myeloperoxidase
Hoechst
Enlarged merge
b
P<0.0001
****
P<0.0001
****
Released DNA/10^5 PMNs(ng/ml)
2500
2000
1500
1000
500
0
Healthy
AT
Artemis
SAVI
d
P=0.028
*
P=0.0393
*
Plasma Elastase(ng/ml)
400
300
200
100
0
Healthy
AT
Artemis
SAVI

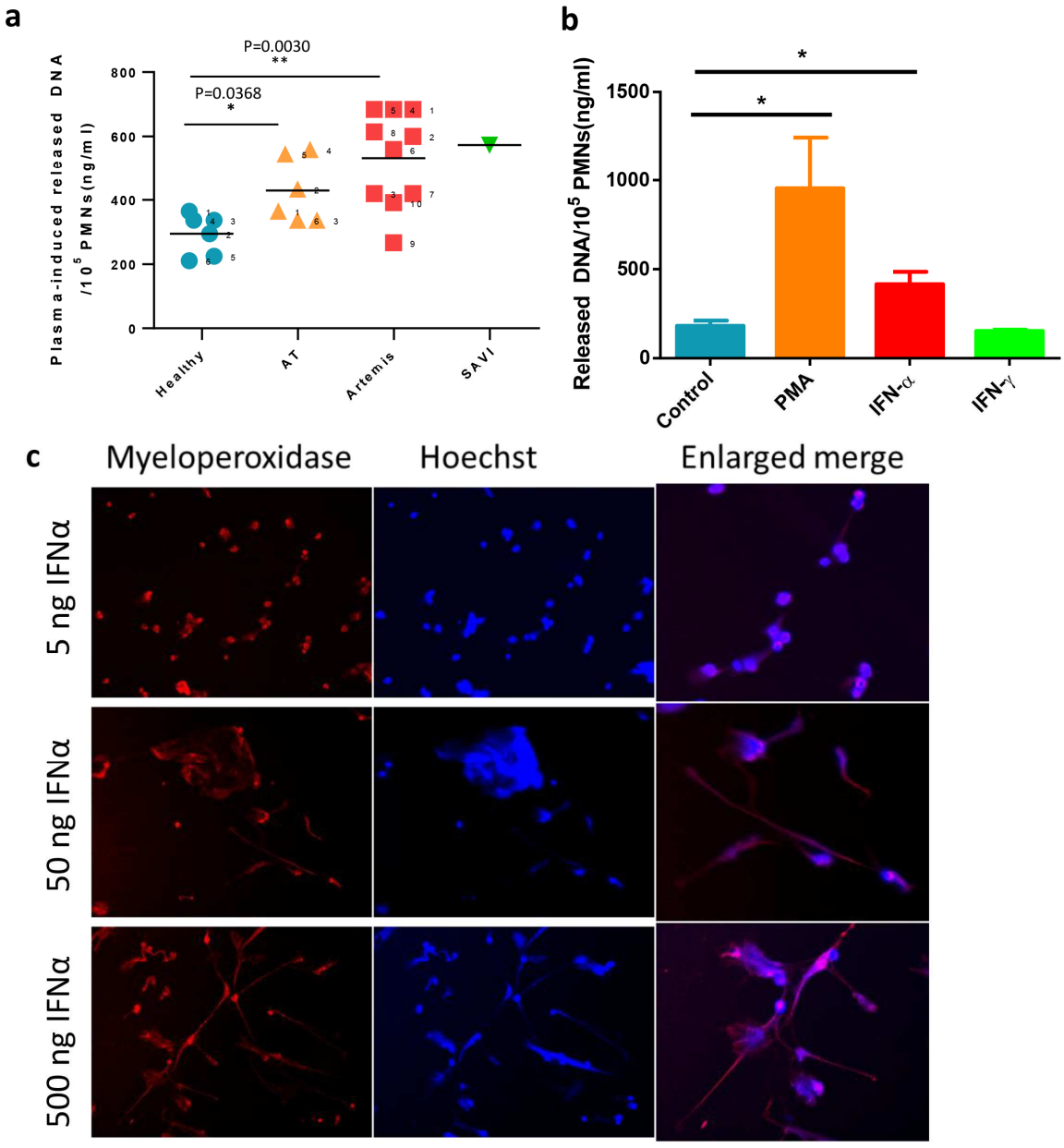
a
P=0.0030
**
P=0.0368
*
Plasma-induced released DNA /10^5 PMNs(ng/ml)
800
600
400
200
0
Healthy
AT
Artemis
SAVI
b
*
*
Released DNA/10^5 PMNs(ng/ml)
1500
1000
500
0
Control
PMA
IFN-α
IFN-γ
c
Myeloperoxidase
Hoechst
Enlarged merge
5 ng IFNα
50 ng IFNα
500 ng IFNα

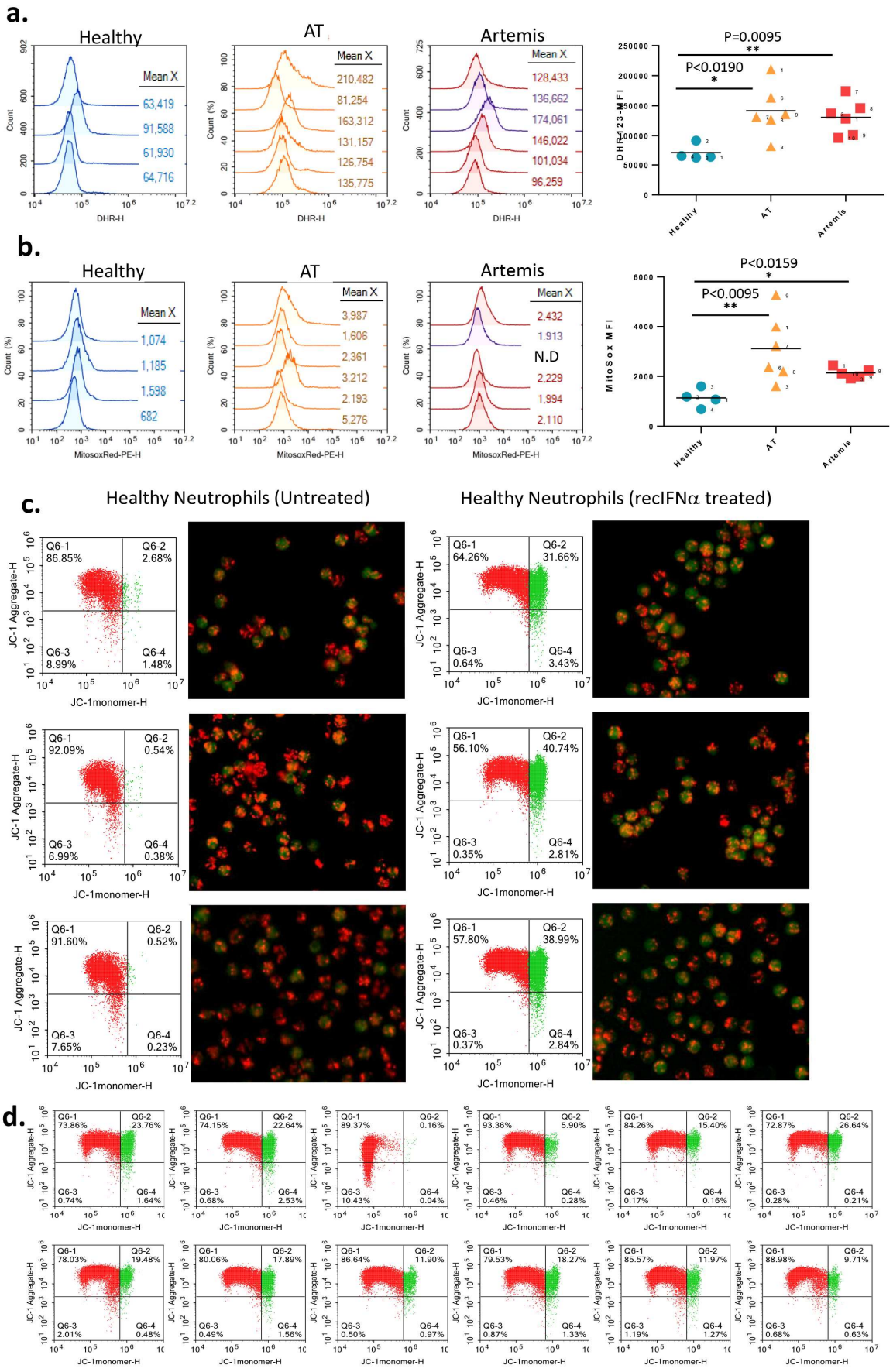
a.
Healthy
AT
Artemis
Mean X
63,419
91,588
61,930
64,716
210,482
81,254
163,312
131,157
126,754
135,775
128,433
136,662
174,061
146,022
101,034
96,259
DHR-H
Count
Count (%)
P=0.0095
**
P<0.0190
*
DHR 123 - MFI
Healthy
AT
Artemis
b.
Healthy
AT
Artemis
Mean X
1,074
1,185
1,598
682
3,987
1,606
2,361
3,212
2,193
5,276
2,432
1.913
N.D
2,229
1,994
2,110
MitosoxRed-PE-H
Count (%)
P<0.0159
*
P<0.0095
**
MitoSox MFI
Healthy
AT
Artemis
c.
Healthy Neutrophils (Untreated)
Healthy Neutrophils (recIFNα treated)
Q6-1
Q6-2
Q6-3
Q6-4
86.85%
2.68%
8.99%
1.48%
64.26%
31.66%
0.64%
3.43%
92.09%
0.54%
6.99%
0.38%
56.10%
40.74%
0.35%
2.81%
91.60%
0.52%
7.65%
0.23%
57.80%
38.99%
0.37%
2.84%
JC-1 Aggregate-H
JC-1monomer-H
d.
73.86%
23.76%
0.74%
1.64%
74.15%
22.64%
0.68%
2.53%
89.37%
0.16%
10.43%
0.04%
93.36%
5.90%
0.46%
0.28%
84.26%
15.40%
0.17%
0.16%
72.87%
26.64%
0.28%
0.21%
78.03%
19.48%
2.01%
0.48%
80.06%
17.89%
0.49%
1.56%
86.64%
11.90%
0.50%
0.97%
79.53%
18.27%
0.87%
1.33%
85.57%
11.97%
1.19%
1.27%
88.98%
9.71%
0.68%
0.63%

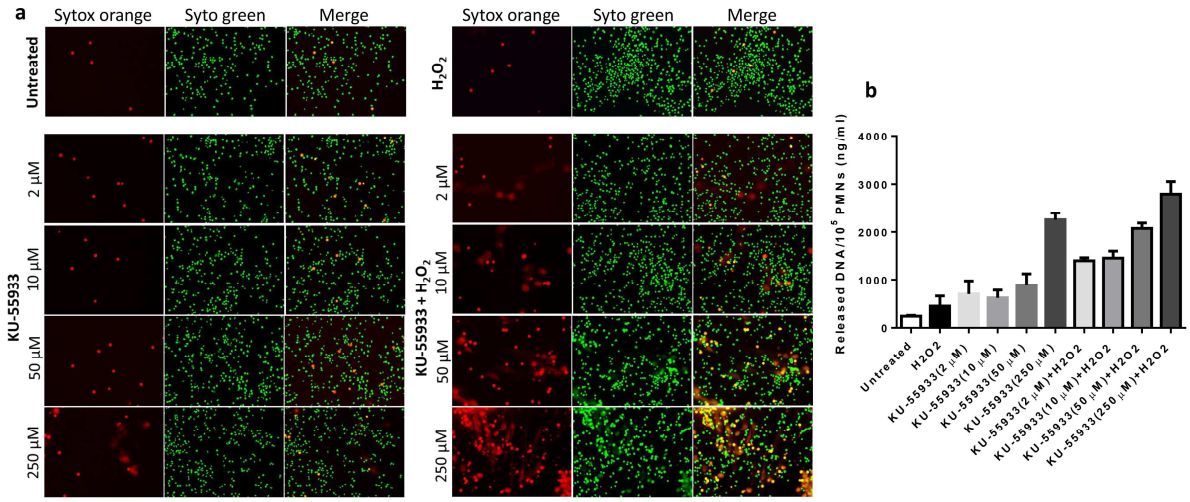

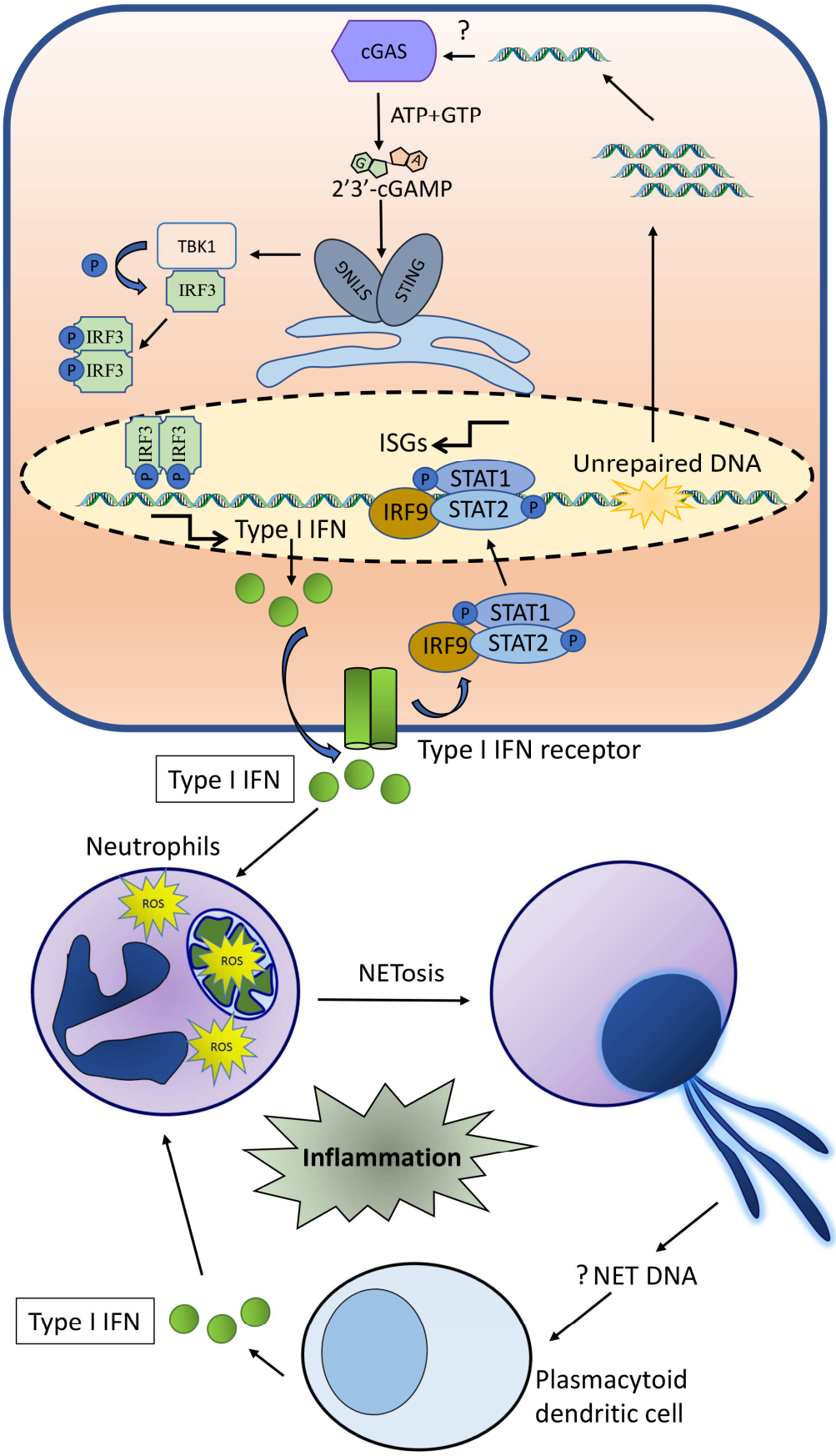
cGAS
?
ATP+GTP
2'3'-cGAMP
TBK1
IRF3
P
IRF3
P
IRF3
STING
STING
ISGs
Unrepaired DNA
IRF3
IRF3
P
P
STAT1
IRF9
STAT2
P
Type I IFN
STAT1
IRF9
STAT2
P
Type I IFN receptor
Type I IFN
Neutrophils
ROS
ROS
ROS
NETosis
Inflammation
? NET DNA
Type I IFN
Plasmacytoid
dendritic cell

Mutation: N154S (c.461A>G)

SAVI patient

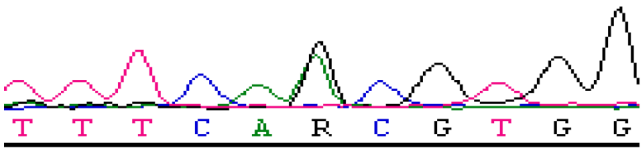

Mother

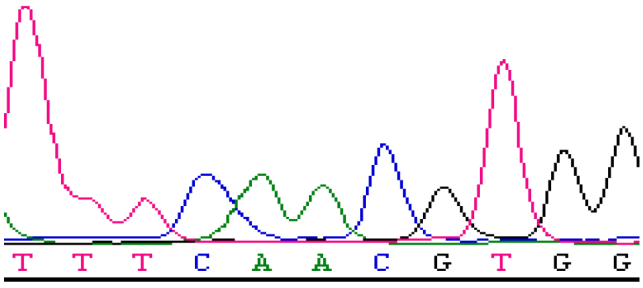

Father

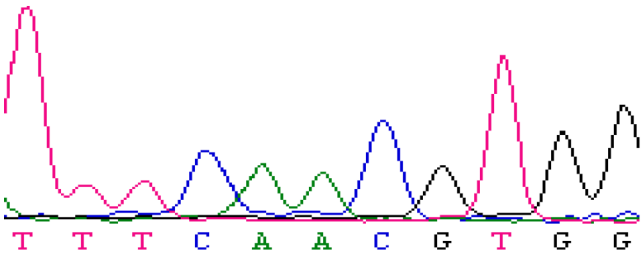

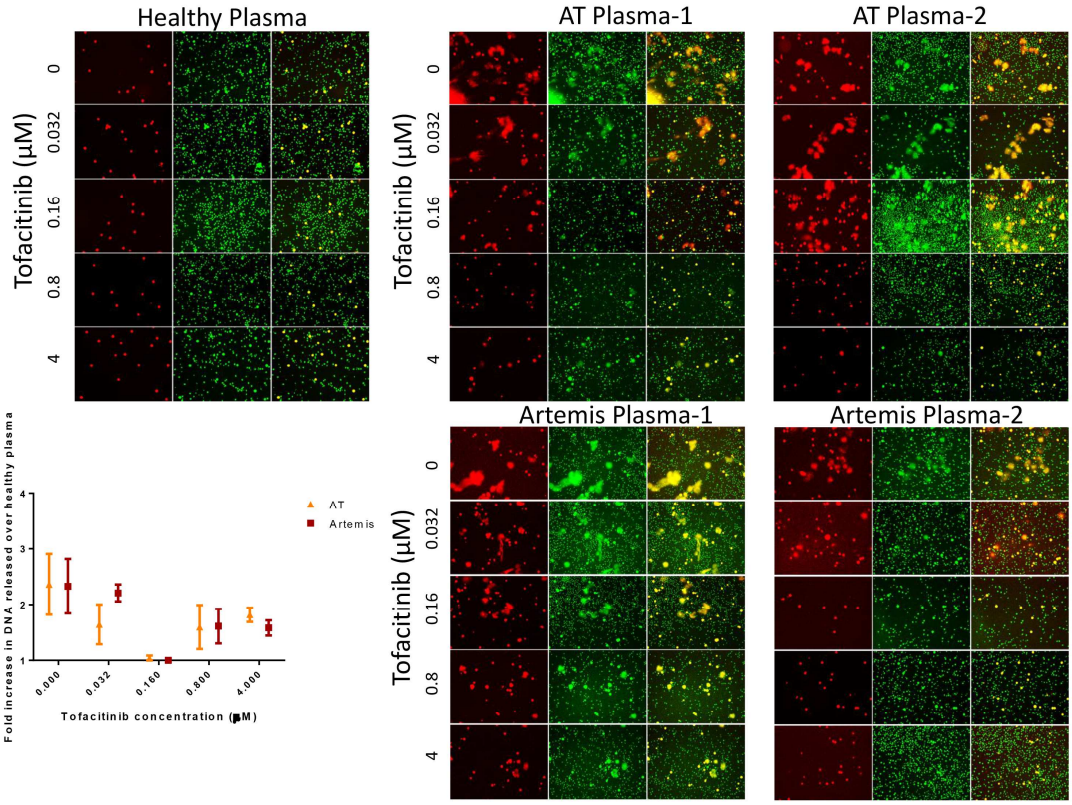

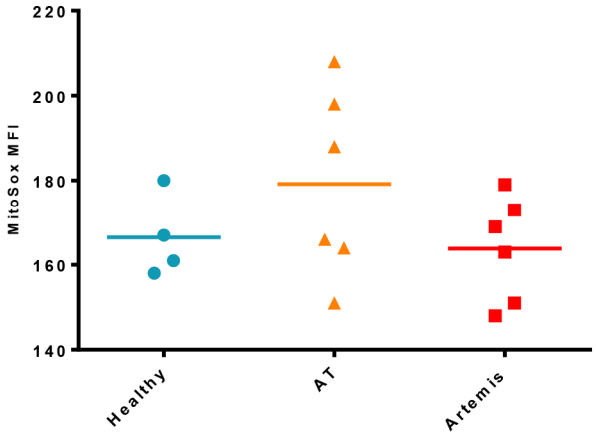

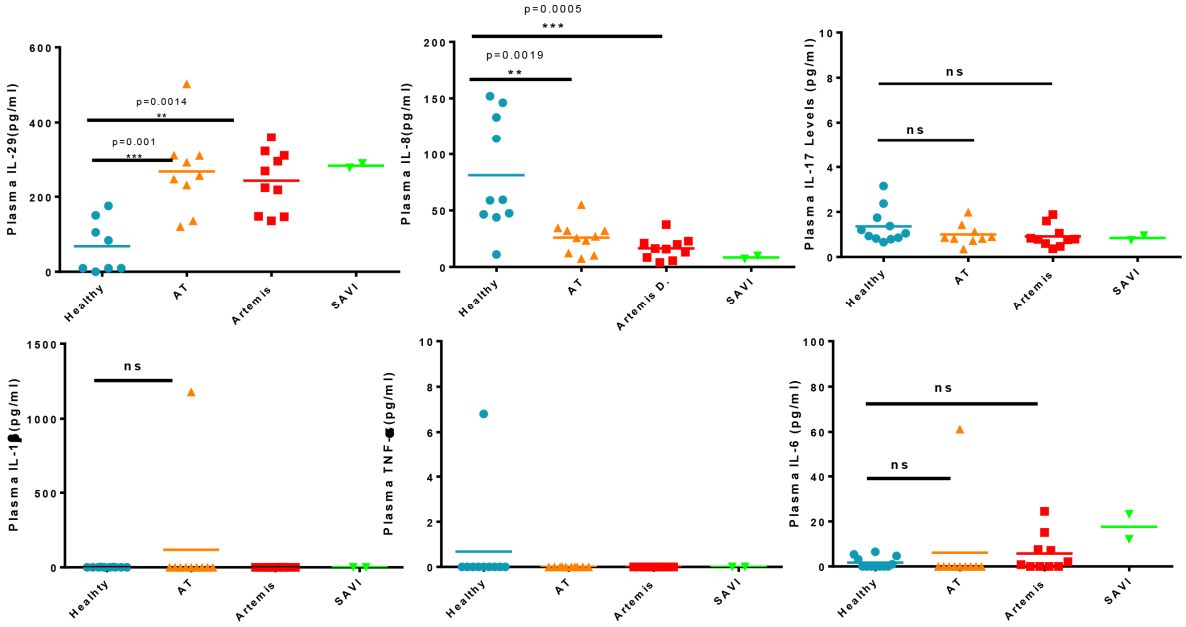

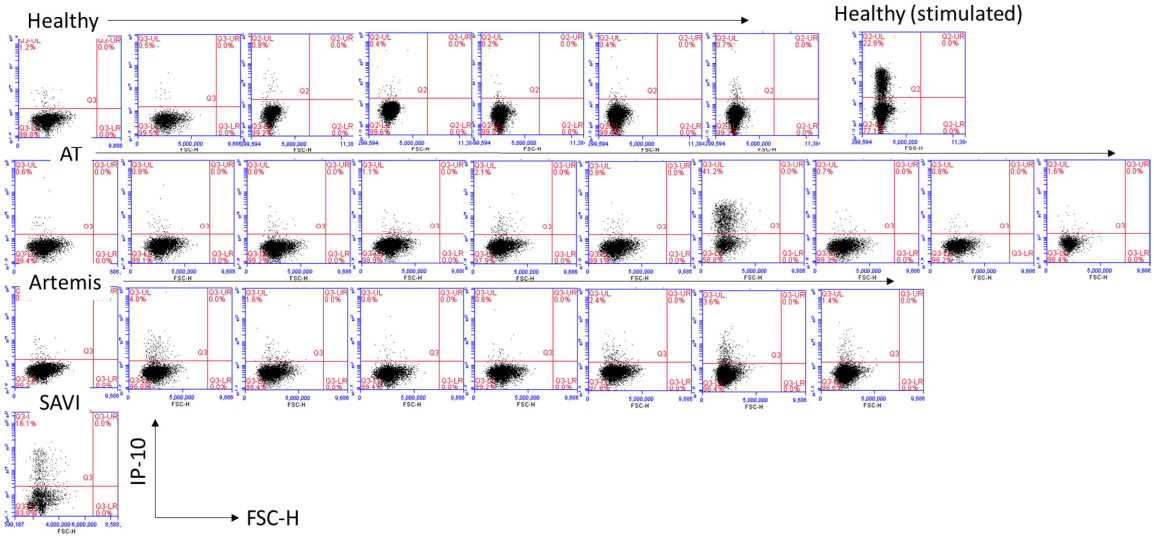

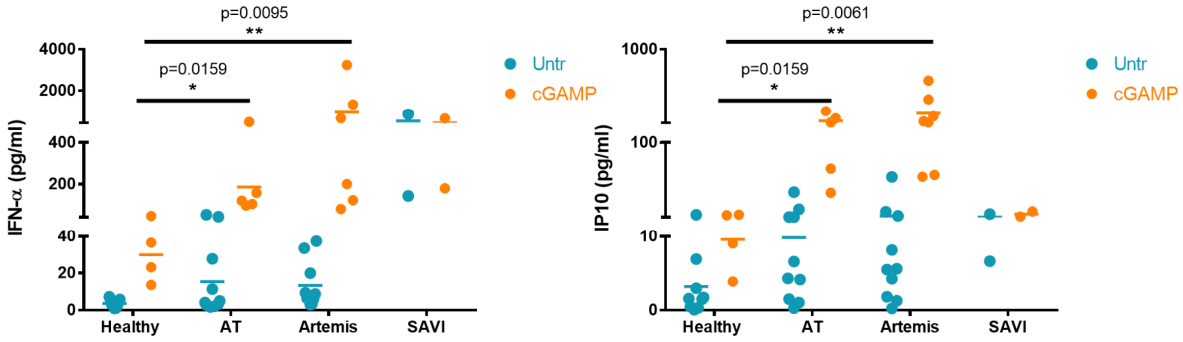

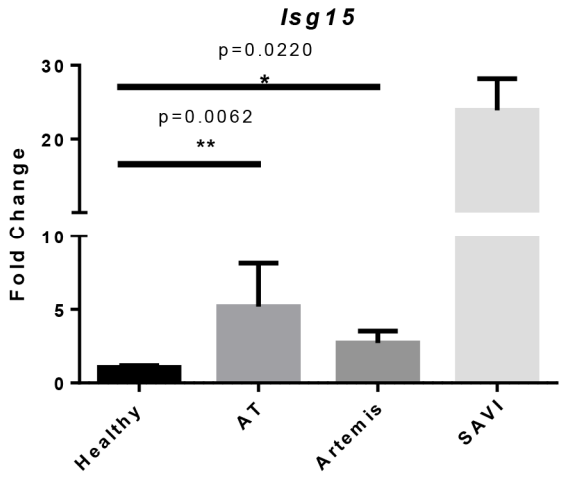

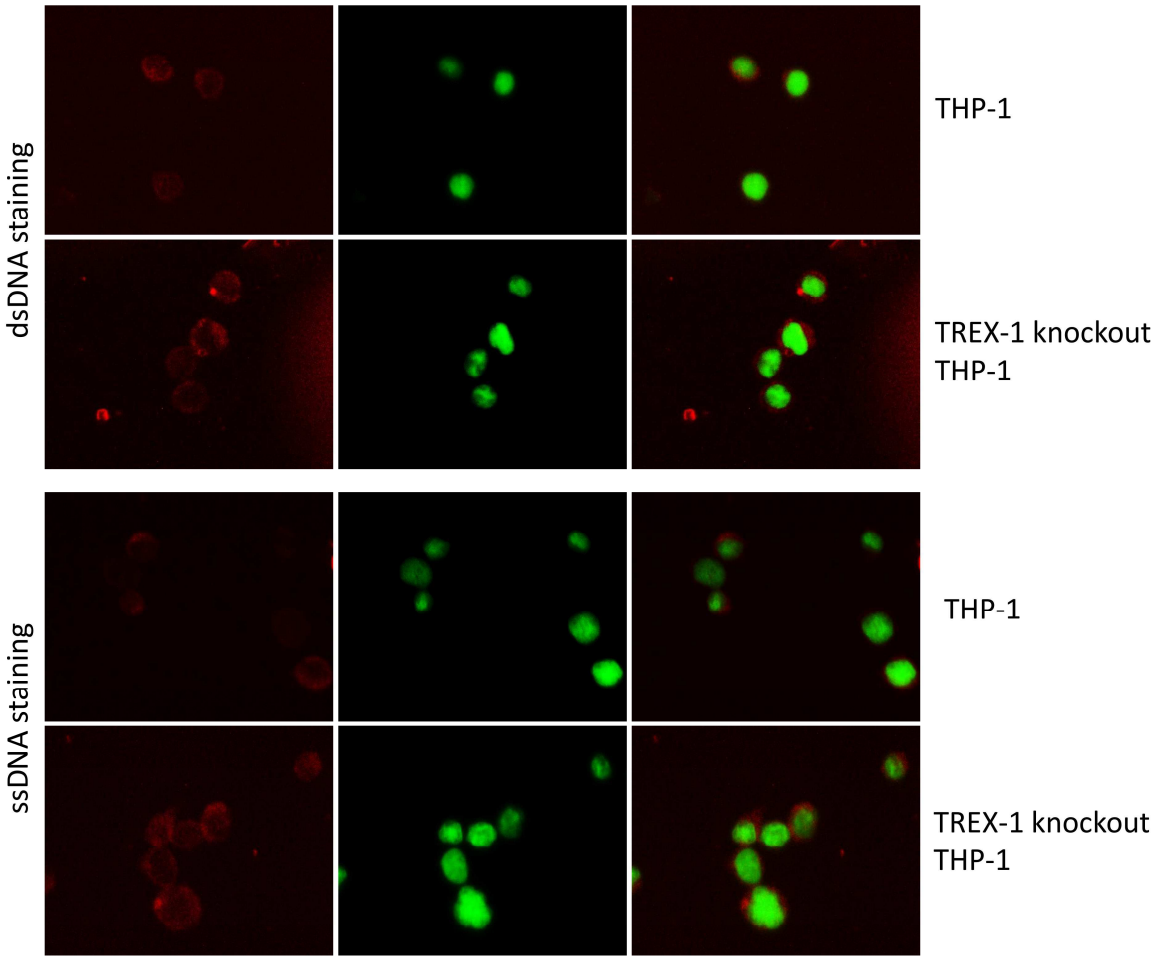
dsDNA staining
THP-1
TREX-1 knockout
THP-1
ssDNA staining
THP-1
TREX-1 knockout
THP-1

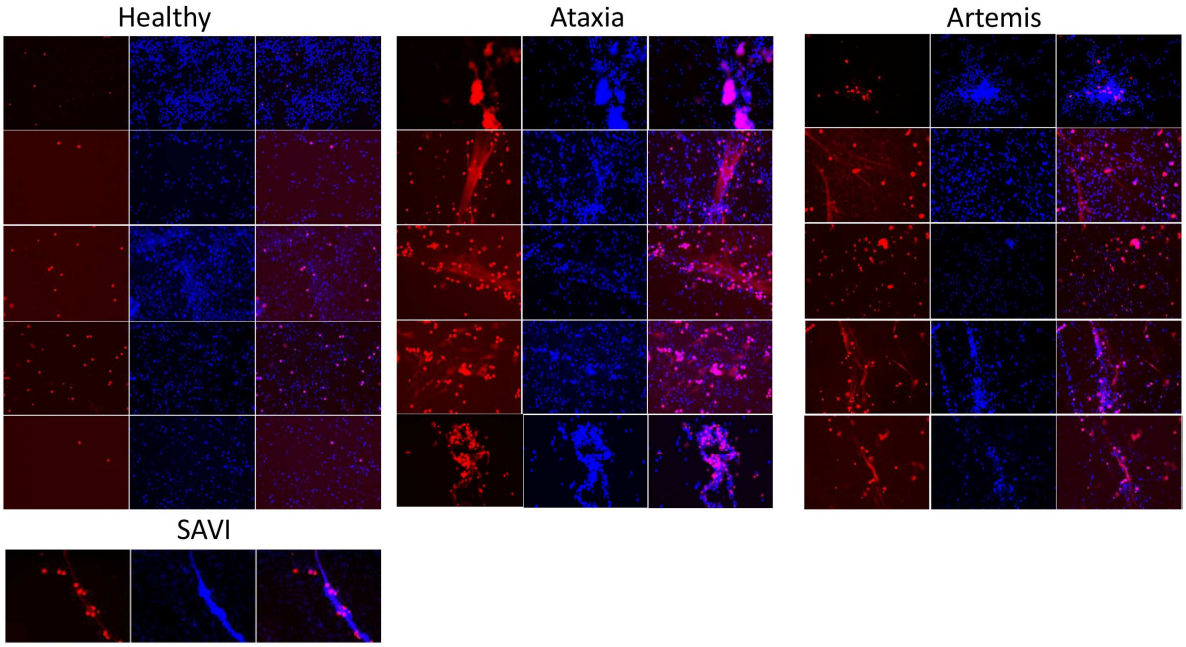

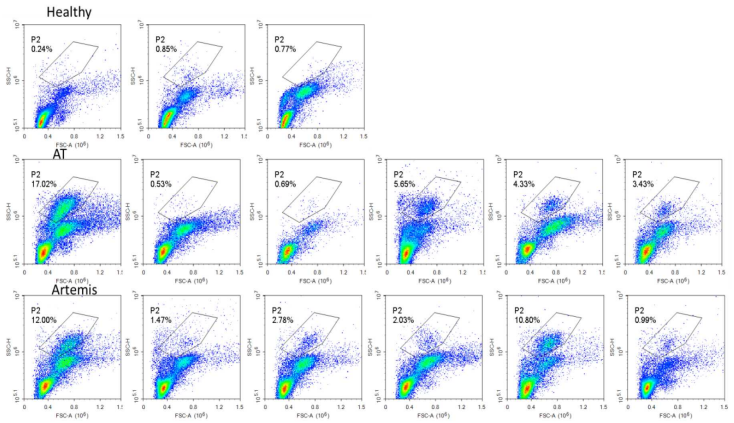

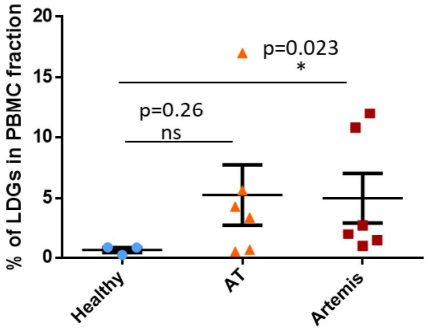

Healthy Neutrophils + Healthy plasma

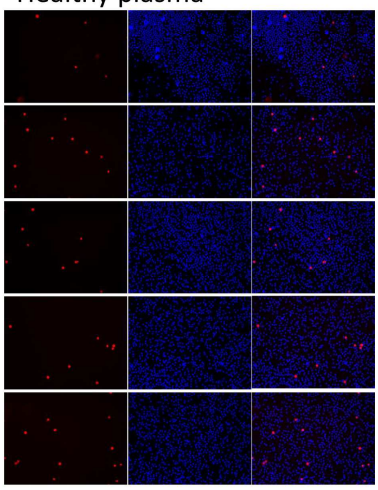

Healthy Neutrophils + AT plasma

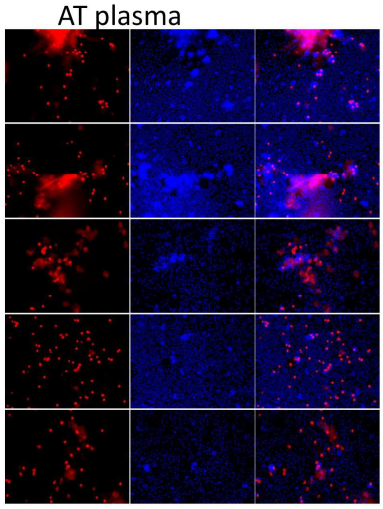

Healthy Neutrophils + Artemis deficient plasma

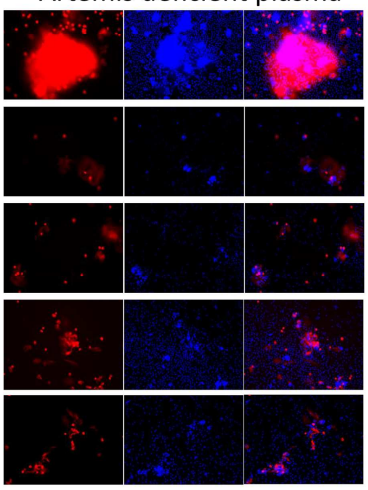

Healthy Neutrophils + SAVI plasma

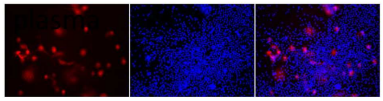

Supplementary Methods

List of Antibodies

Alexa Fluor® 488 Anti-Human-pStat1 (pY701) (Clone 4a, BD Biosciences); PE Anti-Human-IP10 (Clone 6D4/D6/G2, BD Biosciences); Anti-DNA Antibody, single stranded (Clone TNT-3, Merckmillipore); Anti-DNA Antibody, double stranded, (Clone AE-2, Merckmillipore); PE Goat anti-mouse IgG (minimal x-reactivity) (Clone Poly4053, Biolegend); Anti-VDAC1 goat polyclonal (N-18; Santa Cruz Biotechnology, Inc.); Anti-Lamin A/C mouse monoclonal (Leica Biosystems); Anti-β-actin mouse monoclonal (8H10D10, Cell Signaling Technlogy); HRP-Anti-goat IgG (Abcam); HRP-Anti-mouse IgG (Cell Signaling Technology).

Genetic analysis of the SAVI patient

Peripheral venous blood was obtained from the patient and his parents. Genomic DNA was extracted from blood samples using the QIAamp DNA Blood Mini Kit (Qiagen) according to the manufacturer's instructions. Exons (3–8) of the TMEM173 gene were amplified by PCR as previously described (19). For direct DNA sequence analysis, succesfully amplified PCR products were purified using ExoSAP-IT (Thermo Fisher Sci.) according to the manufacturer's protocol. Purified PCR amplicons were sequenced with the same primers used for PCR amplifications in both directions using BigDye Terminator chemistry and analyzed on an ABI 3100 Genetic Analyzer (Applied Biosystems) according to the manufacturer's instructions. The presence of mutations in the TMEM173 (NM_198282) gene was analyzed from the sequencing data using Lasergene SeqMan II (V5.08) software (DNAStar Inc.).

Functional Analyses on patient Samples

Isolation of PBMCs from Whole Blood

Blood samples (5-20 ml) from donors were collected into sodium citrate, or EDTA containing vacutainers. In order to isolate peripheral blood mononuclear cells (PBMCs), Lympho-Paque Cell Separation Medium (Genaxxon Bioscience, Germany) was used. Peripheral blood samples were first diluted 1:1 with PBS and then 3 volumes of blood-PBS mixture was slowly layered onto 2 volumes of separation medium and centrifuged for 30 min at 400 x g at room temperature (RT). Plasma samples were collected from the upper layer, clarified by centrifugation at 2000 x g for 10 min, and stored at -80°C for cytokine analyses and NETosis assays. Mononuclear cells were transferred into sterile 50 ml falcon tubes and washed 3 times in medium (RPMI-1640 supplemented with 2% FBS). PBMC pellets were re-suspended in pre-warmed RPMI-1640 containing 10% FBS.

Isolation of Neutrophils from Blood

Following PBMC isolation and aspiration of density gradient medium, remaining red blood cell+granulocyte pellets were resuspended in a volume of PBS equal to the initial blood volume and then mixed with an equal volume of 3% dextran/PBS (w/v). Tubes were incubated in an upright position for 30 min at RT until a clean interface between RBCs and granulocytes was observed. Upper layers (granulocytes) were then transferred into new tubes, washed with cold PBS and centrifuged for 8 min at 250 x g at 4℃. Supernatants were removed and residual RBCs were lysed by incubation in 2 ml ACK Lysing Buffer (Lonza, Switzerland) for 5 min at RT. Cells were washed with cold PBS two more times (8 min at 250 x g at 4℃). Final pellets containing PMNs were re-suspended in RPMI-1640 supplemented with 5% FBS that was previously inactivated at 65°C for 1 h to ensure DNAse inactivation.

Cytokine Measurements

For determination of circulating cytokine/chemokine levels, plasma samples from healthy subjects, Artemis deficient, AT and SAVI patients were used. To assess cytokines secreted from PBMCs, 400,000 cells were transferred into 96-well flat bottom plates without or with stimulant (10 µg/ml 2'3'-cGAMP) in a total volume of 200 µl, followed by incubation for 24 h. Cell culture supernatants were collected and stored at -20°C. Concentrations of IP-10, IL-8, IL-6, IL-1β and TNFα in plasma or culture supernatants were detected using Cytometric Bead Array (CBA) flex sets (BD Biosciences, USA) according to manufacturer's instructions. Concentration of IFNα in patient and healthy plasma samples was detected using IFNα LumiKine ELISA (Invivogen, USA). Levels of IL-29 (IFN-λ1) and IL-17 in plasma samples were detected by using the IL-29 and IL-17A ELISA Kits (Mabtech, USA). Intracellular IP-10 levels in healthy or patients PBMCs were detected by intracellular cytokine staining. Briefly, $1x10^6$ PBMCs were left untreated or transfected with HSV60 DNA (5 µg/ml complexed with lipofectamine 2000) and incubated for 5 hours at 37°C. At the end of the 5 hours, brefeldin A (10 µg/ml) was added and cells were incubated for 2 more hours. Following fixation with 4% paraformaldehyde, samples were permeabilized and stained in 100 µl permeabilization medium (Medium B, Thermo Fisher Scientific, USA), containing 1 µg/ml anti-human-IP10-PE Ab (Clone 6D4/D6/G2 BD Biosciences, USA). CBA samples and samples for intracellular IP-10 were analyzed on BD Accuri C6 or NovoCyte (Acea Biosciences Inc) flow cytometers. Results of CBA tests were analysed using the FCAP array software version 3.0 (BD Biosciences).

Plasma Elastase Quantitation

For detection of elastase levels in plasma of healthy and patient subjects, human elastase ELISA kit from HycultBiotech (USA) was used according to manufacturer's instructions.

qRT-PCR Analysis of Gene Expression

Total RNAs from PBMCs were extracted using TRIzol (ThermoFisher Scientific, USA). cDNAs were synthesized from 500 ng of total RNAs using the ProtoScript® First Strand

cDNA Synthesis Kit (New England BioLabs, UK). MX1 and ISG15 encoding transcript levels were quantified by qRT-PCR using the SsoAdvanced™ Universal SYBR® Green Supermix (BioRAD, USA) and the MX1 and ISG15 primers from Invivogen (USA). The results were normalized to the β-actin housekeeping gene and expressed as fold change relative to RNA samples from healthy controls using the comparative CT method (ΔΔCT).

Quantitation of STAT1 Phosphorylation

PBMCs ($1x10^6$/ml) were either left untreated or treated with recombinant IFNα (5-500 ng/ml) for 20 minutes and then fixed in 4% paraformaldehyde. Cells were then permeabilized using 95% ice-cold methanol (10 minutes on ice) and washed twice with PBS/BSA (5%). Cells were stained with Alexa 488 conjugated anti-human pSTAT1 (pY701) (BD Biosciences, USA) antibody for 45 minutes, washed twice in PBS/BSA and analyzed on a NovoCyte Flow Cytometer (ACEA Biosciences, USA) using the 488 nm blue laser for excitation and the BL1 channel (530/30 nm filter) for detection.

Cytosolic DNA Staining

Isolated patient and healthy PBMCs ($5x10^6$ cells) were plated in 6-well flat bottom plates. Cells were either untreated or treated with UVB light at a distance of 1 cm for 15 min using the Transilluminator 2000 (Bio-Rad Laboratories, 312 nm wavelength). After incubation for 6h at 37℃, cells were fixed with 4% paraformaldehyde, treated with 80% ice-cold methanol for 10 minutes and washed twice with FACS buffer containing 3% BSA. The cells were then stained either with anti-ssDNA or anti-dsDNA antibodies (1µg/ml each; Merck, Germany) for 30 minutes and washed twice with FACS buffer. Then, the cells were stained with PE conjugated goat anti-mouse IgG secondary antibody (Biolegend, USA) for 30 minutes and washed twice afterwards. The cells were then either visualized using the Floid Cell Imaging Station (ThermoFisher Scientific, USA) or analyzed by flow cytometry. For flow cytometry, a 488 nm blue laser was used for excitation and the BL2 channel (572/28 nm filter) was used for detection. For microscopic analysis, excitation was achieved using a LED light source (586/15) and fluorescence was captured using a 646/68 filter. Images were collected under a fixed 20X Plan Fluorite objective with a Numerical Aperture (NA) = 0.45.

Preparation of cytosolic extracts from PBMCs and amplification of cytosolic mitochondrial/nuclear DNA by qPCR

Cytoplasmic extracts of patient and healthy PBMCs were prepared using NE-PER nuclear and cytoplasmic extraction reagents (Thermo Fisher Scientific, USA) according to the manufacturer's protocol. Whole cell extracts (WCE), mitochondrial and nuclear extracts were prepared from HCT116 cell line (ATCC-CCL-247) as described previously (65). Protein concentrations of the cell extracts were determined by the Bradford method with BSA as standard (Bio-Rad Protein Assay, Bio-Rad Laboratories, USA). The purity of the cytoplasmic extracts was confirmed by western blotting of the cytoplasmic extracts, WCE, nuclear and mitochondrial extracts. Briefly, the cell extracts

(1.5 µg) were mixed with 2xSDS sample buffer (Bio-Rad Laboratories, USA) containing β-mercaptoethanol and heated at 95 °C for 5 min. Then, the extracts were resolved on 4-20% Criterion Tris-HCl protein gel and transferred to PVDF membranes (0.2-µm pore size) (Bio-Rad Laboratories, USA). The immunoblots were analyzed with following primary antibodies: mouse anti-Lamin A/C (dilution 1:200), goat anti-VDAC1 (dilution 1:1000) and mouse anti-β-actin (dilution 1:1000) and then secondary antibodies were employed: HRP-conjugate ab goat (dilution 1:5000) and HRP-linked antibody mouse (dilution 1:5000). The immunoblots were visualized using Amersham ECL Plus (GE Healthcare, USA) and ChemiDoc Imaging sytstems (Bio-Rad Laboratories, USA).

Cytosolic DNA was purified using QIAquick nucleotide removal kit (Qiagen, USA) according to the manufacturer's protocol. qPCR analysis of cytosolic DNA was performed using FastStart essential DNA green master kit (Roche Diagnostics, USA) as suggested by the manufacturer's instructions and analyzed using LightCycler Nano system (Roche Diagnostics). Samples were denatured by heating at 95℃ for 5min followed by 40 cycles of amplification (95℃ for 20 s, 58℃ and 72℃ for 20s). Primers used in qPCR analysis were as follows: mitochondrial ND5 primer, 5'-CCGGAAGCCTATTCGCAGGA-3' and 5'-ACAGCGAGGGCTGTGAGTTT-3' (fragment length: 103 bp) and nuclear H3 primer, 5'-TACCATGGCTCGTACAAAGCAG-3' and 5'-CCTGTAACGATGAGGTTTCTTCAC-3' (fragment length: 133 bp). The threshold cycle number (Ct) values of ND5 and H3 were determined for each sample. qPCR products were also electrophoresed on 1% agarose gel containing ethidium bromide in 1XTBE and visualized by ChemiDoc Imaging sytstems (Bio-Rad Laboratories, USA). Thermo Scientific GeneRuler 100 bp DNA ladder was used on agarose gel electrophoresis.

Imaging of Neutrophil Extracellular Traps (NETs)

Neutrophils (80,000 cells/well) were seeded onto 96-well flat bottom plates and were left untreated or were treated with PMA as a neutrophil extracellular trap (NET) inducer (50 ng/ml) or with recombinant IFN-α (5-500 ng/ml). In another set of experiments, neutrophils from healthy donors were treated with either healthy or patient plasma samples (20%). Stimulations and incubations were carried out in RPMI-1640 supplemented with 2% DNAse inactivated FBS. After 5h incubation at 37℃, cells were stained with NucBlue (ThermoFisher Scientific, USA), and 5 µM SYTOX Orange (ThermoFisher Scientific, USA) for 30 min. For myeloperoxidase staining experiments, same stimulations were performed on poly-l-lysine coated plates but cells were fixed with 4% paraformaldehyde after 5 hours and stained with 1 µg/ml of biotin conjugated anti-MPO antibody (HycultBiotech, USA) for 30 minutes followed by 2X washing in PBS. Cells were then stained with PE-streptavidin (1 µg/ml; BD Bioscience, USA) for 30 minutes, washed twice with PBS and finally stained with NucBlue or SytoGreen for 20 minutes. Samples were then visualized using the Floid Cell Imaging Station (ThermoFisher Scientific, USA). During imaging, wells were screened carefully and representative images were captured from each well. Images were then analyzed using

the LSM Image Browser software (Zeiss, Germany). For microscopic analysis, excitation and fluorescence capture was achieved using the following LED light sources and capture filters: Excitation: 390/40 (Blue), 482/18 (Green), 586/15 (Red); Capture: 46/33 (Blue), 532/59 (Green), 646/68 (Red). Images were collected under a fixed 20X Plan Fluorite objective with a Numerical Aperture (NA) = 0.45.

Quantification of Neutrophil Extracellular Traps (NETs)

200,000 neutrophils were transferred to 96-well flat bottom plates and were left untreated or treated with PMA as a neutrophil extracellular trap (NET) inducer (50 ng/ml) or treated with recombinant IFN-α (5-500 ng/ml). In another set of experiments, neutrophils from healthy donors were treated with either healthy or patient plasma samples (20%). Stimulations and incubations were carried out in RPMI-1640 supplemented with 2% DNAse inactivated FBS. After 5h incubation at 37℃, samples were treated with 500 mU/ml of micrococcal nuclease (New England BioLabs, UK) in 50 µl nuclease buffer for 30 min at 37℃ and the reaction was terminated using 5 mM EDTA. Plates were then centrifuged at 200 x g for 5 min and supernatants were collected into new plates and stored at -80℃ for quantification with Picogreen. For quantification of released neutrophil extracellular traps (NETs), Quant-iT Picogreen dsDNA Assay Kit (ThermoFisher Scientific, USA) was used according to manufacturer's instructions. Briefly, 100 µl of supernatants were transferred into separate black, opaque, flat-bottomed 96-well plates, and Picogreen reagent was diluted 1:200 in TE Buffer (freshly made). Diluted Picogreen reagent was then added onto supernatants. After 2-5 min incubation at RT in dark, amount of extracellular DNA was quantified using a standard curve based on known concentrations of lambda DNA (0.1-10 µg/ml). Fluorescence values were recorded on a Synergy HT Microplate Reader (BioTek, China) using excitation/emission settings of 485/20 and 525/20.

Detection of ROS and Mitochondrial Stress in Neutrophils

For cytosolic reactive oxygen species (ROS) determination, healthy or patient neutrophils ($1x10^6$/ml,) were either untreated or treated with PMA (50ng/ml) for 30 minutes. After 30 minutes, cytosolic ROS was detected by adding 2.5 µg/ml of Dihydrorhodamine 123 (DHR123) (ThermoFisher Scientific, USA) onto the cells, followed by incubation for 15 minutes and washing twice with PBS. The cells were then analyzed flow cytometrically. For mitochondrial ROS determination, healthy or patient neutrophils ($1x10^6$/ml) were either untreated or treated with recombinant IFNα (500 ng/ml) for 30 minutes in the presence of 5 µM MitosoxRed (ThermoFisher Scientific, USA). The cells were then washed and analyzed by flow cytometry. For JC-1 staining, healthy or patient neutrophils ($1x10^6$/ml) were either untreated or treated with recombinant IFNα (500 ng/ml) for 30 minutes and then the cells were stained with JC-1 (Cayman Chemical, USA) according to manufacturer's instructions and analyzed microscopically under the Floid Cell Imaging Station or flow cytometrically.

Statistical Analysis

For statistical analysis, Mann Whitney U-test was used to compare healthy vs. patient groups. For all comparisons, 95% confidence intervals were used and P values of <0.05 were considered significant. All analyses were carried out using the GraphPad Prism 6.1 (GraphPad Software Inc., USA) software.

Supplementary Figures

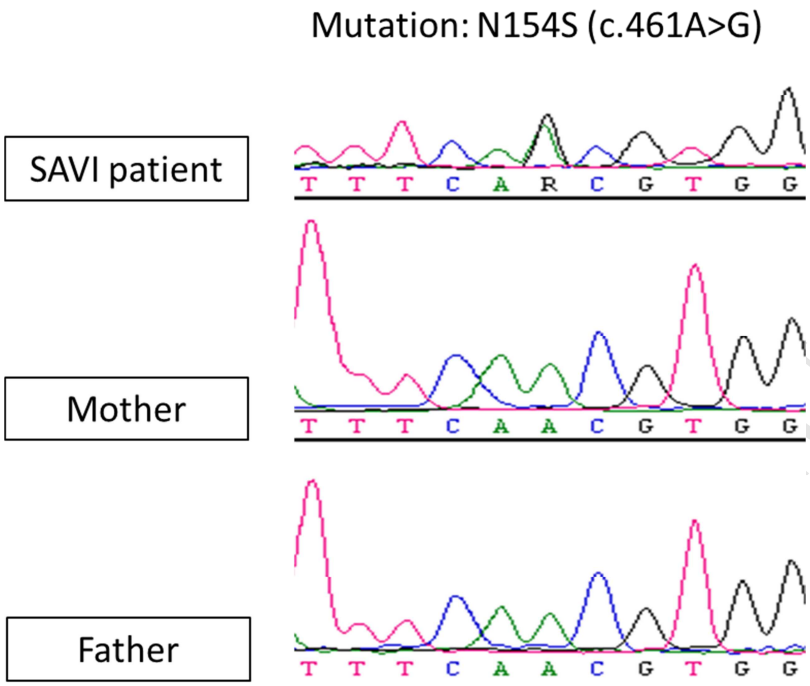

Supplementary Figure S1. Sequencing electropherogram of SAVI patient and his parents. Sequencing electropherogram of exon V of the TMEM173 gene shows a heterozygous A>G mutation at position 461. All 6 Exons (Exons 3,4,5,6,7 and 8) were subjected to targeted sequencing with no detectable mutations in any of the exons apart from exon V.

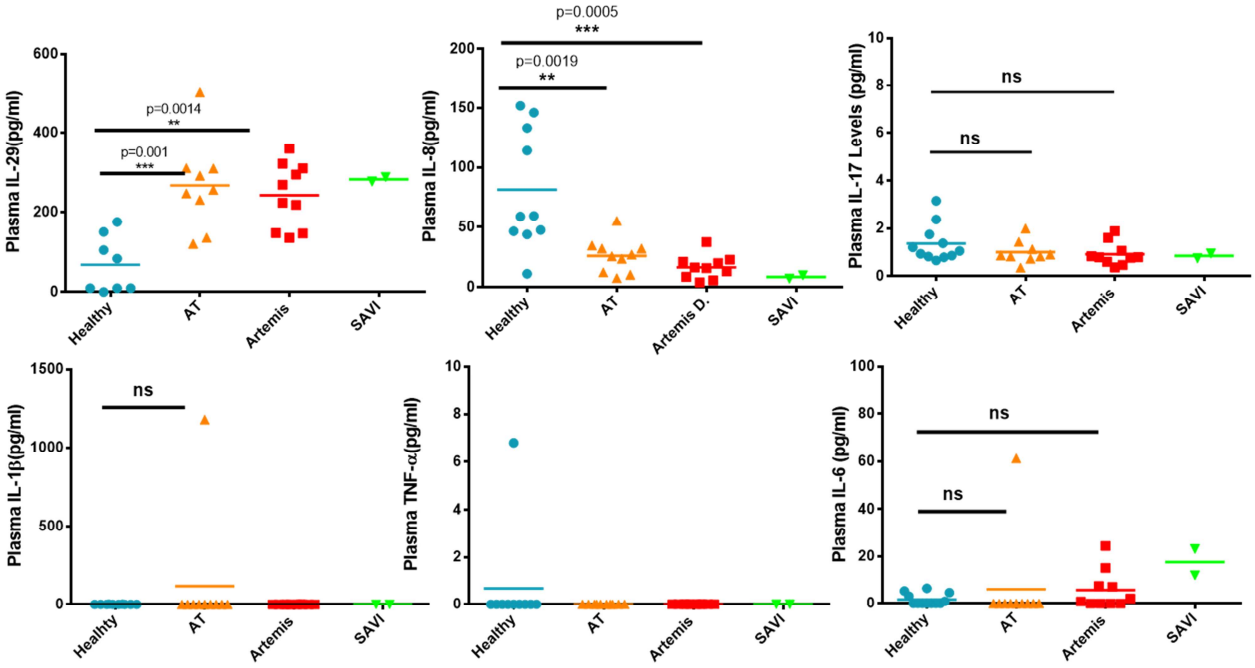

Supplementary Figure S2. Plasma cytokine levels in Healthy subjects and patients. Plasma IL-29 (Interferon λ1) levels were significantly higher in AT, Artemis deficient and SAVI patients. Circulating levels of the pro-inflammatory cytokines were either detected by ELISA (IL-29 and IL-17) or by cytometric bead array (IL-8, IL-1β, TNFα and IL-6).

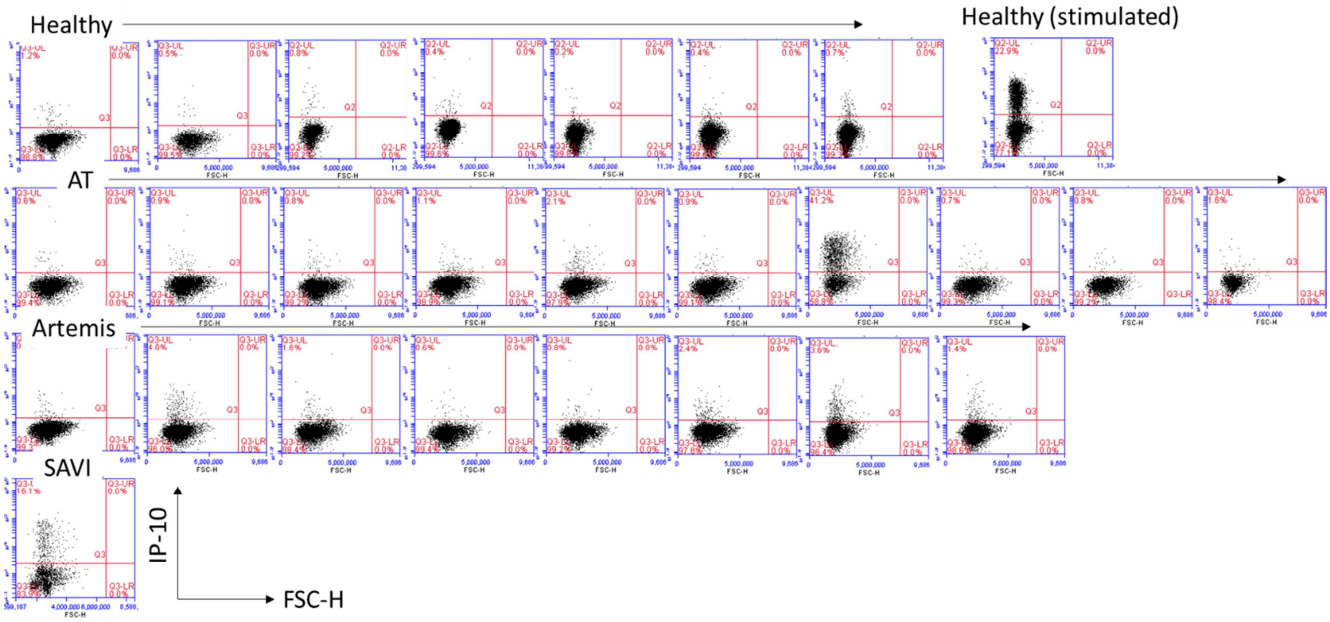

Supplementary Figure S3. Intracellular cytokine staining for spontaneous IP-10 production in PBMCs. Healthy and patient PBMCs were incubated 7 h (with brefeldin A addition during the last 2 h of incubation) in the absence of any stimulation.Cells were then stained for IP-10 and analyzed by Flow cytometry. In some experiments HSV60 immune stimulatory DNA was transfected to cells as a positive control (depicted as Healthy stimulated in the uppermost plot).

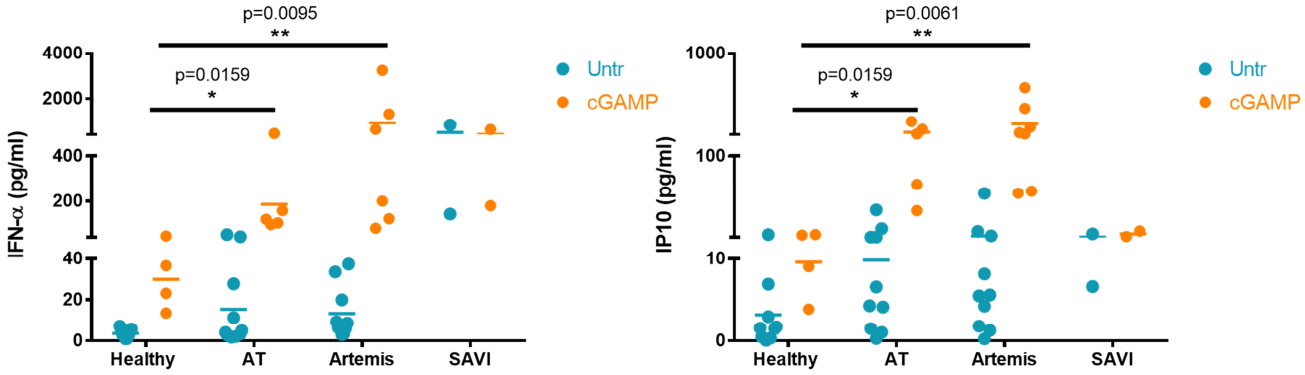

Supplementary Figure S4. IFNα and IP-10 secretion from PBMCs stimulated with the STING ligand 2'3'-cGAMP. AT and Artemis deficient patient cells respond more robustly to stimulation with cGAMP than healthy controls. SAVI patient's cells do not respond to further stimulation with cGAMP, consistent with published results (19). PBMCs isolated from patients and healthy donors (2 x 10^6/ml) were incubated with or without cGAMP (10 µg/ml) for 24 h, supernatants were collected and assessed for IFNα or IP-10 production by cytometric bead array. Following flow cytometric analysis of bead samples and standards, pg/ml concentrations were calculated using the FCAP software. Statistical significance was determined using the Mann-Whitney U-test.

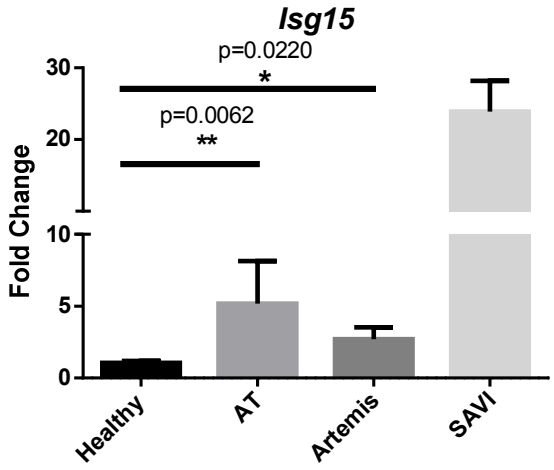

Supplementary Figure S5. Expression levels of ISG15 in PBMCs. Patient PBMCs express elevated levels of the interferon stimulated gene ISG15 when compared to healthy controls. 500 ng of total RNAs purified from PBMCs were converted to cDNAs using the ProtoScript® First Strand cDNA Synthesis Kit. ISG15 expression was quantified by qRT-PCR using the SsoAdvanced™ Universal SYBR® Green Supermix (BioRAD, USA) ISG15 primers from Invivogen (USA). The results were normalized to the β-actin housekeeping gene and expressed as fold change relative to RNA samples from healthy controls using the comparative CT method (ΔΔCT).

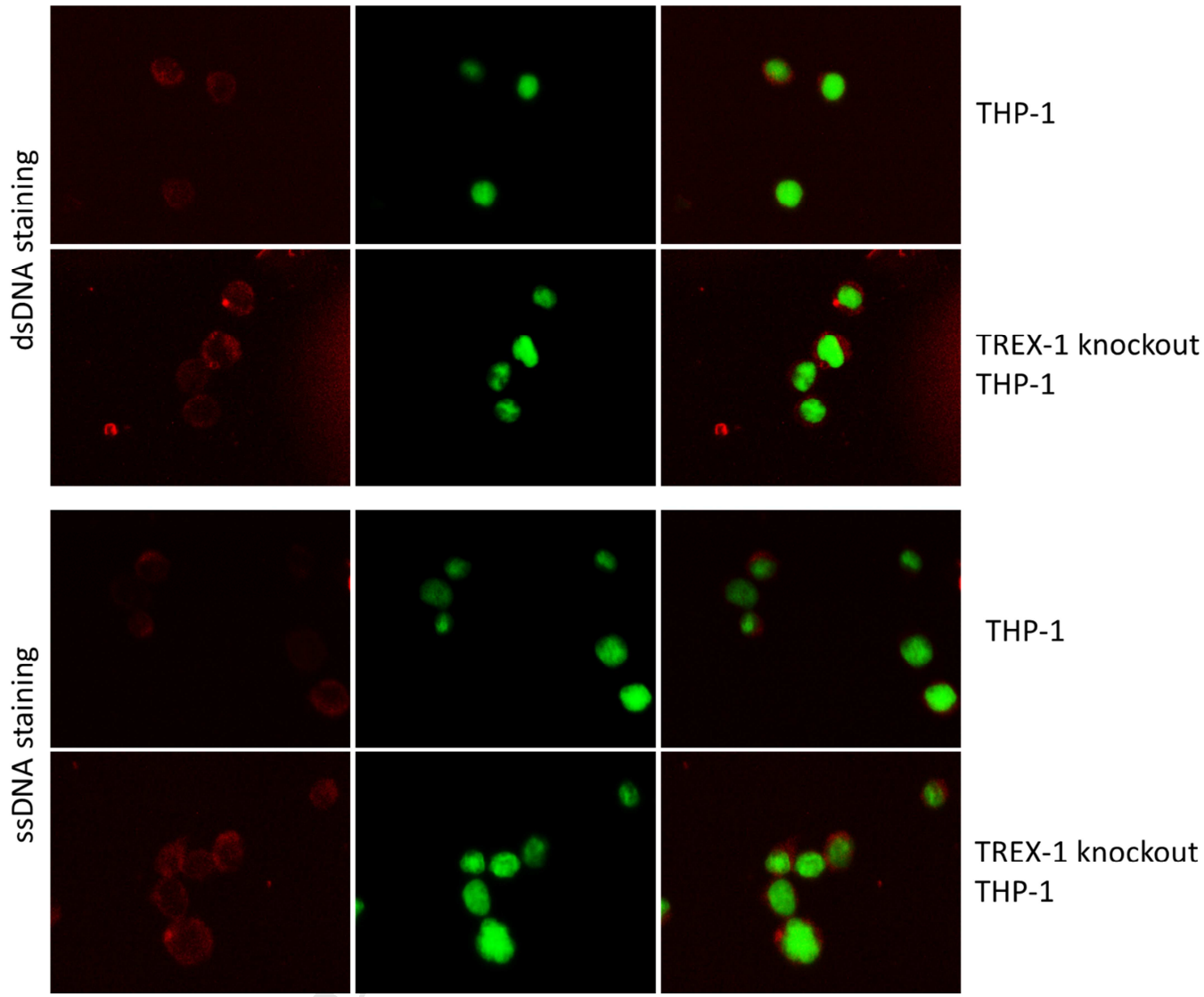

Supplementary Figure S6. Specificity of anti-ssDNA and anti-dsDNA staining protocol. Results show that neither the ssDNA- nor the dsDNA-specific antibody localize to the nucleus as shown by the absence of the red antibody signal within the green stained nuclei. As expected, the intensities of cytosolic nucleic acid signals were higher in TREX-1 deficient cells when compared to their wild type controls.

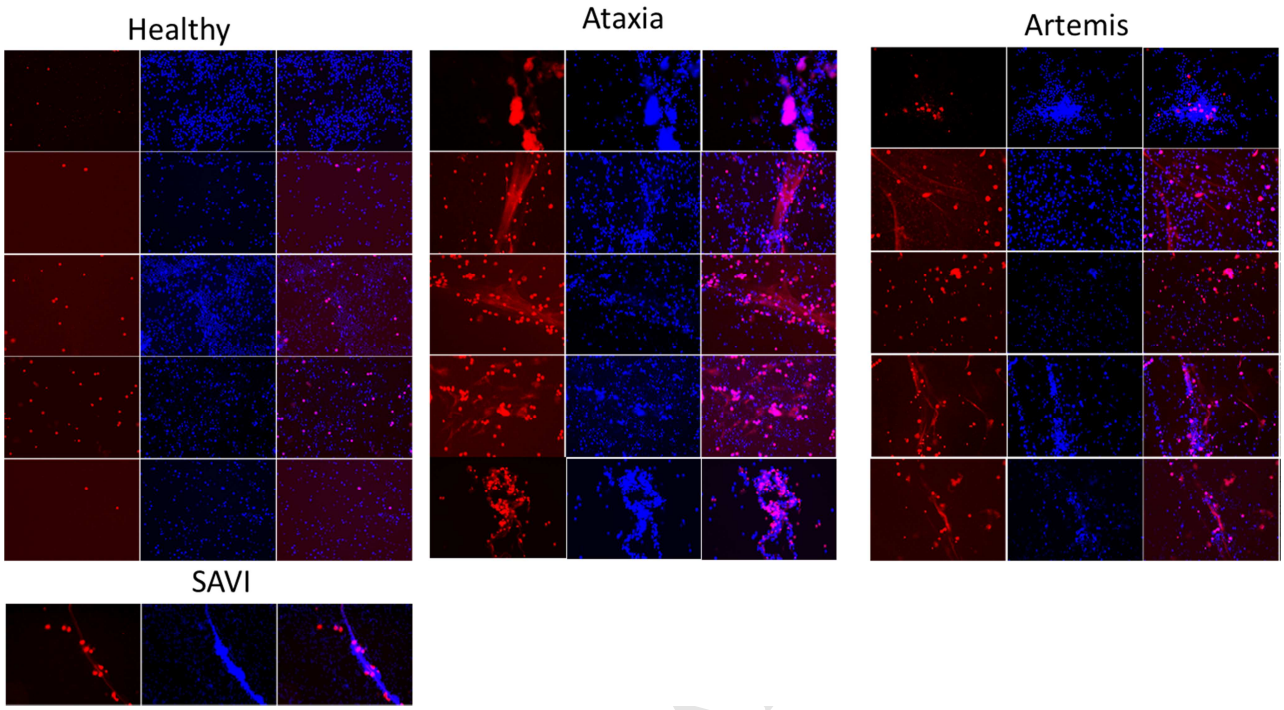

Supplementary Figure S7. Unprimed patient neutrophils spontaneously produce neutrophil extracellular traps (NETs). NET images from 5 different healthy, AT and Artemis deficient subjects and from the SAVI patient demonstrate the presence of spontaneous NET formation in patient but not healthy neutrophils. NETs were imaged 5 h after plating of freshly isolated neutrophils (80,000 cells/200 µl) following staining with Sytox Orange (5 µM) for extracellular DNA (red) and Hoechst (20 µl) (blue) for both extracellular and intracellular DNA.

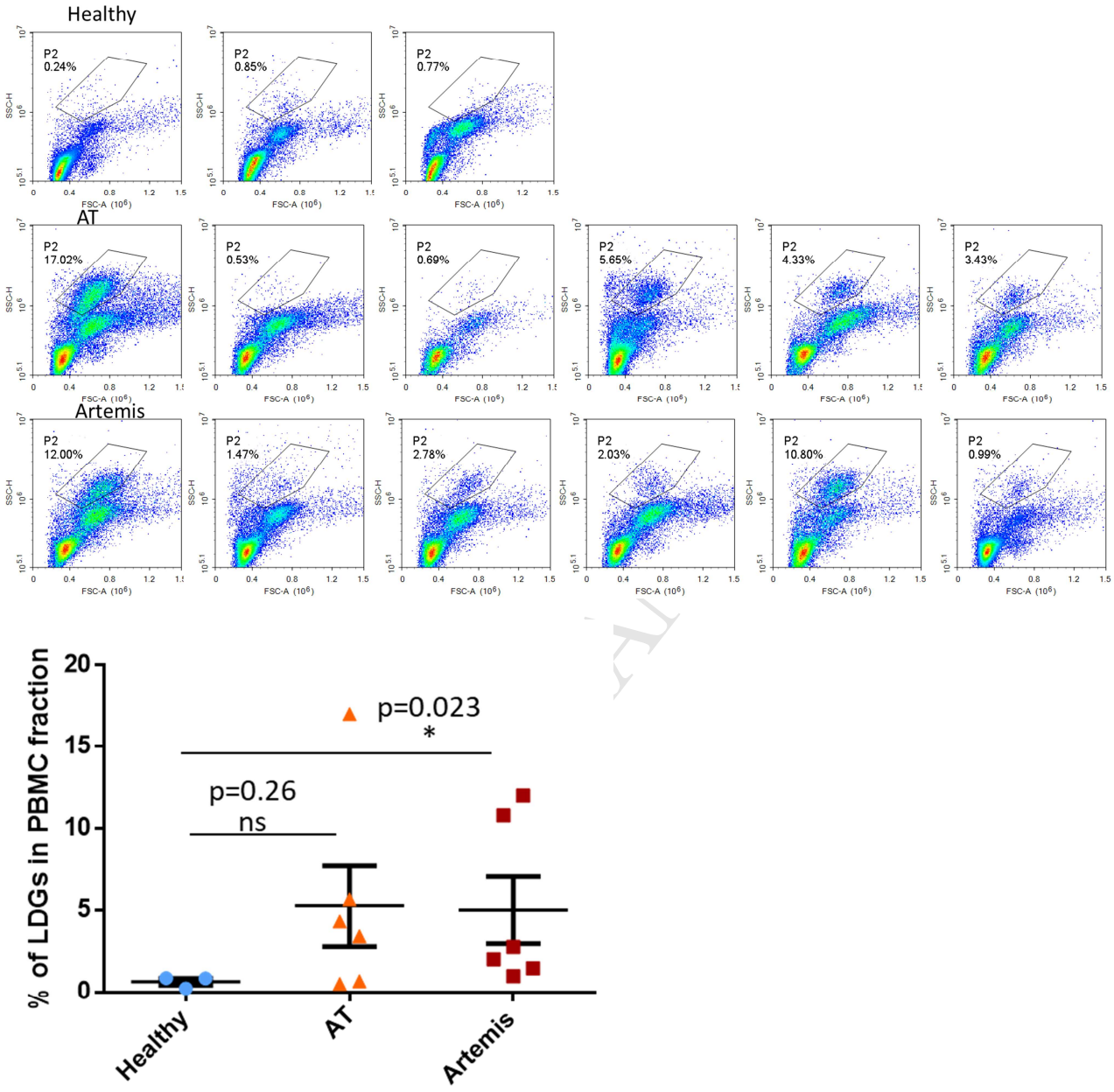

Supplementary Figure S8. Percent of low-density granulocytes in PBMC fractions. Cells within the PBMC fractions that displayed high side scatter (SSC-H) were gated and their percentages are presented.Significance among groups was analyzed using the Mann Whitney U test.

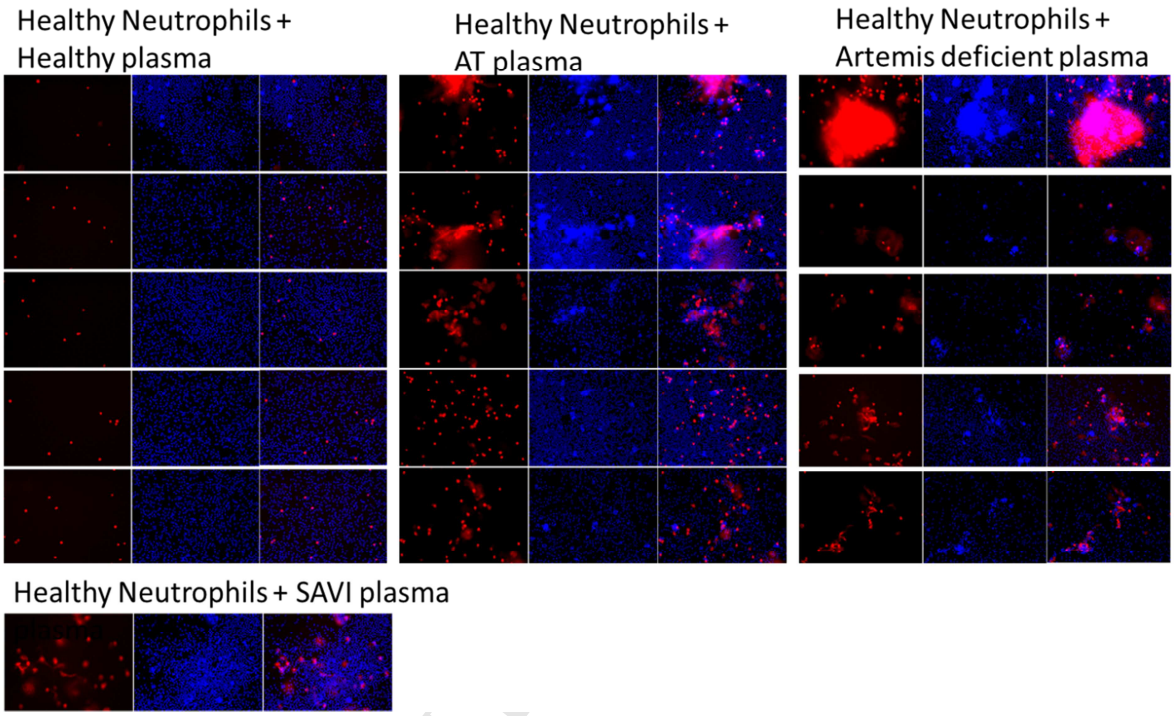

Supplementary Figure S9. Plasma of AT, Artemis deficient and SAVI patients trigger NETosis in healthy neutrophils. Healthy PMNs were incubated with plasma obtained from 5 healthy, 5 AT, 5 Artemis deficient or 1 SAVI patient. Microscopy images were taken 5 h later following staining of cells with Sytox orange for extracellular DNA (red) and Hoechst (blue) for both extracellular and intracellular DNA.

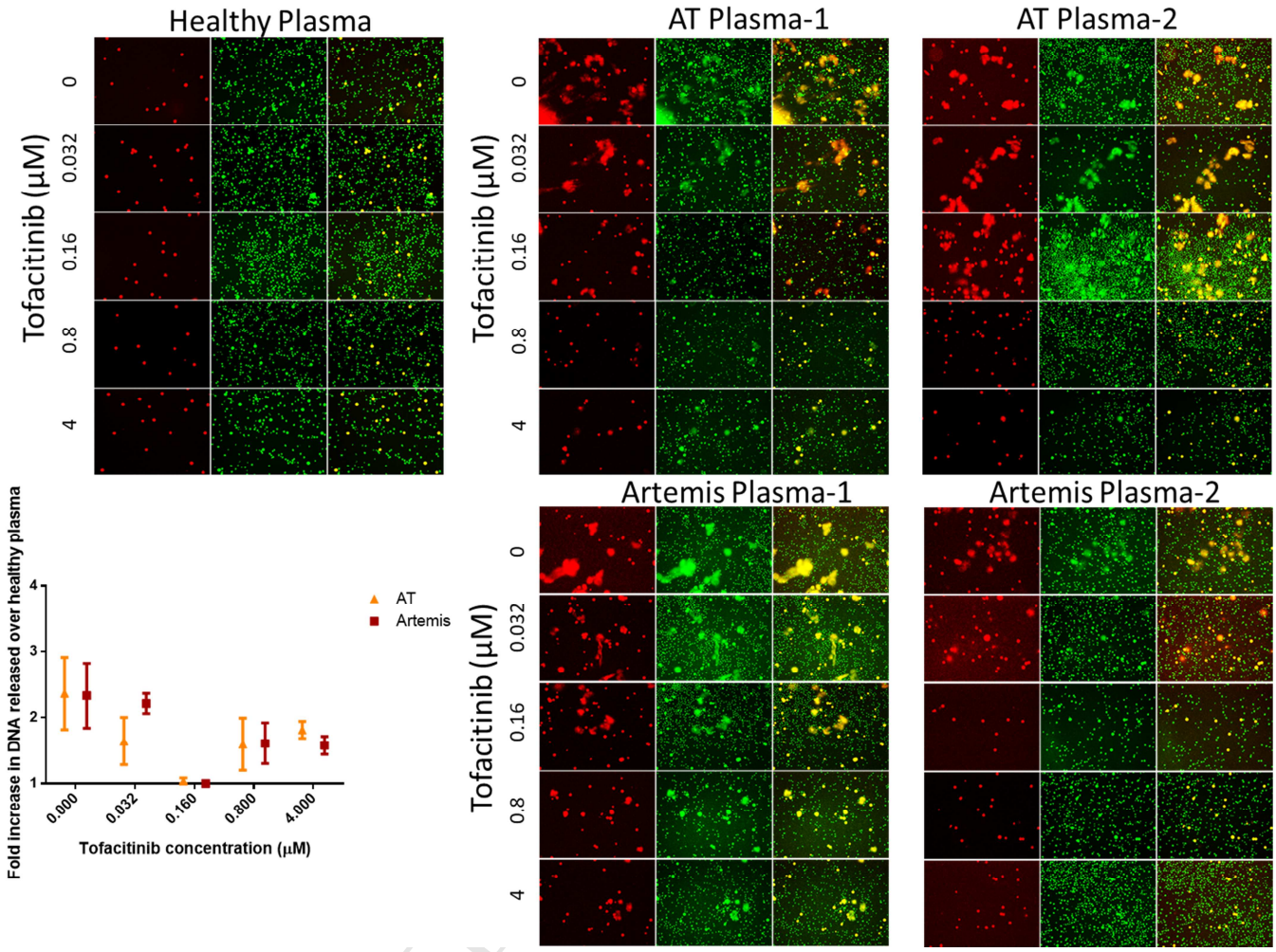

Supplementary Figure S10. AT and Artemis deficient patient plasma-induced NETosis in healthy neutrophils is suppressed in the presence of Tofacitinib. Healthy PMNs were pre-incubated without or with the JAK inhibitor Tofacitinib (0-4 µM) for 30 min followed by incubation with plasma obtained from a healthy donor, AT or Artemis deficient patients. Microscopy images were taken 5 h later following staining of cells with Sytox orange for extracellular DNA (red) and Syto green (green) for both extracellular and intracellular DNA. For quantitative analysis of extruded DNA, MNAse/picogreen based method was used.

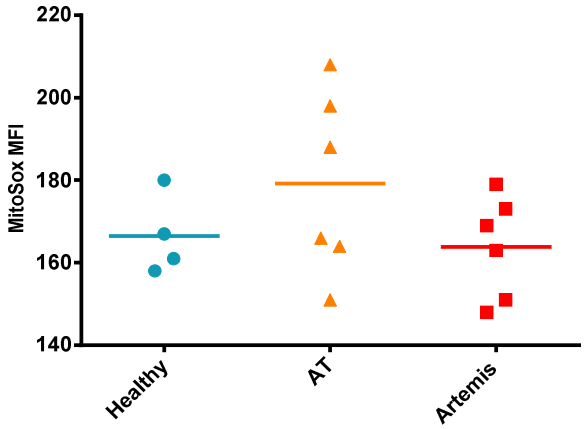

Supplementary Figure S11. MitoSOX Red staining of unstimulated neutrophils. Mitochondrial ROS was undetectable in unstimulated neutrophils.

Supplementary Table 1. Clinical Characteristics of AT, Artemis deficient and SAVI Patients

Patients and clinical characteristics	Artem1	Artem2	Artem3	Artem4	Artem5	Artem6	Artem7	Artem8	Artem9	Artem10
Year of birth	2011	2009	2006	2004	1994	1994	2009	2005	2011	2009
Gender	F	M	F	F	F	F	M	F	M	F
Age of onset	2y	2y	5y	2y	4y	10y	4y	4y	10 mo	-
Mutation	exon3 c.194C>T/ exon 3 c.194C>T	exon3 c.194C>T/ exon 3 c.194C>T	exon3 c.194C>T/ exon 3 c.194C>T	exon3 c.194C>T/ exon 3 c.194C>T	exon3 c.194C>T/ exon 3 c.194C>T	exon3 c.194C>T/ exon 3 c.194C>T	exon3 c.194C>T/ exon 3 c.194C>T	exon3 c.194C>T/ exon 3 c.194C>T	exon3 c.194C>T/ exon 3 c.194C>T	exon3 c.194C>T/ exon 3 c.194C>T
Infections (Lower respiratory tract infections=LRTI; Upper respiratory tract infections=URTI; Otitis media=OM; gastroenteritis=GE)	URTI	URTI	URTI, LRTI	LRTI, OM, URTI, GE	URTI, LRTI, GE, OM	URTI, LRTI	URTI	LRTI, Severe varicella infection, Brucellosis	URTI	no infections
skin lesions (violaceous plaques and nodules on face, arms or legs)	aphtous stomatitis, granulomatous skin lesions	granulo-matous skin lesions; wart-like skin lesions	no	no	no	wart-like skin lesions	wart-like skin lesions	wart-like skin lesions	wart-like skin lesions	no
malignancies (ALL=acute lymphocytic leukemia)	no	no	no	no	no	no	no	no	no	pre-pre B ALL
Lung involvement (Bronchiectasis=BE)	BE	-	BE	BE	BE	BE	-	BE	-	-
Autoimmunity	no	no	no	no	no	no	no	no	no	no
Telangiectasia	no	no	no	no	no	no	no	no	no	no
Treatment (Intravenous immunoglobulin substitution=IVIG; Antibiotic prophylaxis=AP; IC=inhaled corticosteroids)	IVIG, AP, IC	IVIG, corticosteroids	IVIG, AP, IC	IVIG, AP	IVIG, AP, oxygen, IC	IVIG, AP	IVIG, AP	IVIG, AP, IC	IVIG, AP	IVIG, AP

Patients and clinical characteristics	AT1	AT2	AT3	AT4	AT5	AT6	AT7	AT8	AT9	AT10
Year of birth	2003	2002	2007	2004	2012	1999	2009	2003	2009	2011
Gender	F	F	M	M	F	F	F	F	M	F
Age of onset	3y	4y	16 /12m	6 m	6 m	1.5 y	2 y	1 y	1 y	1 y
Mutation	ne	ne	ne	exon43 c.6082C>T/ exon43 c.6082C>T	ne	Asn1983Ser Homozygous	ne	Asp1853Asn/ Asp1853Asn	p.X3057S(c.9170G>C) Homozygous	Asp1853Asn/His2872Leu
Infections (Lower respiratory tract infections=LRTI; Upper respiratory tract infections=URTI; Otitis media=OM; gastroenteritis=GE)	URTI LRTI	URTI LRTI	URTI LRTI	URTI LRTI	URTI LRTI GE	URTI LRTI	URTI	URTI LRTI	URTI LRTI	URTI LRTI
skin lesions (violaceous plaques and nodules on face, arms or legs)	no	no	no	no	no	no	no	no	no	no
malignancies (NHL=non-Hodgkin lymphoma)	no	no	no	no	no	no	no	yes (NHL)	no	no
Lung involvement (Bronchiectasis=BE)	BE	BE	-	BE	-	-	-	BE	-	-
Autoimmunity	no	no	no	no	no	no	no	no	no	no
Telangiectasia	yes	yes	yes	yes	no	yes	yes	yes	yes	yes
Treatment (Intravenous immunoglobulin substitution=IVIG; Antibiotic prophylaxis=AP; IC=inhaled corticosteroids)	none	none	none	IVIG AP IC	IVIG AP	IVIG AP	IVIG AP	IVIG AP (EX-December 2015)	IVIG AP	IVIG AP IC

ne: not examined

Patient and clinical characteristics	SAVI
Year of birth	
Gender	male
Age of onset	
Mutation	N154S
Infections (Lower respiratory tract infections=LRTI; Upper respiratory tract infections=URTI; Otitis media=OM; gastroenteritis=GE)	URTI OM
skin lesions (violaceous plaques and nodules on face, arms or legs)	Violaceous plaques Distal ulcerative lesions and acral tissue loss
malignancies (ALL=acute lymphocytic leukemia)	None
Lung involvement (Bronchiectasis=BE)	Interstitial lung disease
Autoimmunity	Low titer, fluctuating autoantibodies
Telangiectasia	yes
Treatment (Intravenous immunoglobulin substitution=IVIG; Antibiotic prophylaxis=AP; IC=inhaled corticosteroids)	none

Supplementary Table 2. Hematological Findings of Patients

Peripheral blood cell counts (1-3)	Artem1	Artem2	Artem3	Artem4	Artem5	Artem6	Artem7	Artem8	Artem9	Artem10
WBC [cells/µl] (age;reference range)	5300 (3y; 4000-10400) (7200)	5300 (5y; 4000-10400) (5400)	7310 (8y; 3700-11100) **(↓ 3100)**	7200 (5y; 4000-10400) **(↑ 15500)**	**↑ 37800** (8y; 3700-11100) **(↑ 14900)**	7650 (18y; 4300-11400) (4700)	7300 (4y; 4000-10400) (6000)	6880 (7y; 3700-11100) (8800)	**↓ 2800** (3y; 4000-10400) **(↓ 3100)**	**↓ 2400** (5y; 4000-10400) **(↓ 1700)**
ALC [cells/µl] (range: 1000-2800)	2000 (1700)	**↓ 800** (1000)	1600 (1000)	1400 (1800)	3780 (1700)	1220 (1100)	**↓ 900** (1100)	2440 **(↓ 500)**	1000 **(↓ 900)**	**↓ 600** **(↓ 600)**
B cells [cells/µl] (age;reference range)	**↓ 17** (3y; 200-2100)	**↓ 22** (5y; 200-1600)	**↓ 13** (8y; 200-1600)	**↓ 193** (5y; 200-1600),	**↓ 118** (8y; 200-1600),	**↓ 24** (18y; 100-500)	**↓ 36** (4y; 200-2100)	**↓ 24** (7y; 200-1600)	**↓ 90** (3y; 200-2100)	**↓ 0** (5y; 200-1600)
T cells [cells/µl] (age;reference range)	**↓ 540** (3y; 900-4500)	**↓ 547** (5y; 700-4200)	**↓ 602** (8y, 700-4200)	**↓ 532** (5y; 700-4200)	1689 (8y; 700-4200),	**↓ 683** (18y; 700-2100)	**↓ 558** (4y; 900-4500)	2025 (7y; 700-4200)	**↓ 490** (3y; 900-4500)	**↓ 390** (5y; 700-4200)
CD4+ T cells [cells/µl] (age;reference range)	**↓ 160** (3y; 500-2400)	**↓ 217** (5y; 300-2000)	**↓ 229** (8y; 300-2000)	**↓ 220** (5y; 300-2000)	695 (8y; 300-2000)	**↓ 268** (18y; 300-1400)	**↓ 207** (4y; 500-2400)	903 (7y; 300-2000)	**↓ 180** (3y; 500-2400)	**↓ 36** (5y; 300-2000)
CD8+ T cells [cells/µl] (age;reference range)	**↓ 240** (3y; 300-1600)	**↓ 268** (5y; 300-1800)	396 (8y; 300-1800)	308 (5y; 300-1800)	1557 (8y; 300-1800)	439 (18y; 200-900)	**↓ 243** (4y; 300-1600)	1000 (7y; 300-1800)	420 (3y; 300-1600)	312 (5y; 300-1800)
NK cells [cells/µl] (age;reference range)	**↑ 1320** (3y; 100-1000)	226 (5y; 90-900)	446 (8y; 90-900)	352 (5y; 90-900)	**↑ 1436** (8y; 90-900)	402 (18y; 90-600)	126 (4y; 100-1000)	240 (7y; 90-900)	320 (3y; 100-1000)	126 (5y; 90-900)
Neutrophils [cells/µl] (1-9y;1500-8500) (10-20y; 1500-8500)	2900 (4400)	**↑ 8590** (3400)	5600 (1700)	4700 **(↑ 12800)**	**↑ 25000** **(↑11800)**	5440 2600	5700 (4000)	3500 (7900)	**↓ 1300** **(↓ 1300)**	**(↓ 800)**

Peripheral blood cell counts	AT1	AT2	AT3	AT4	AT5	AT6	AT7	AT8	AT9	AT10
WBC [cells/µl] (range: 3700-11400)	8100	8200	9800	5700	5800	4300	5400	6300	9300	6200
ALC [cells/µl] (range: 1000-2800)	2500	1100	2200	1700	1800	1700	1200	2100	2500	1400
B cells [cells/µl] (200-1600)	ne	ne	ne	**↓17**	**↓144**	**↓68**	240	**↓21**	200	**↓144**
T cells [cells/µl] (900-4200)	ne	ne	ne	1309	972	**↓833**	**↓672**	1239	975	**↓576**
CD4+ T cells [cells/µl] (300-2000)	ne	ne	ne	850	594	357	408	336	**↓150**	**↓198**
CD8+ T cells [cells/µl] (300-1800)	ne	ne	ne	340	342	663	**↓192**	819	1275	612
NK cells [cells/µl] (90-900)	ne	ne	ne	255	432	680	120	588	**↑1300**	702
Neutrophils [cells/µl] (1-9y;1500-8500) (10-20y; 1500-8500)	4600	5900	6300	3100	3300	1900	3500	3100	5900	3700

ne: not examined

Peripheral blood cell counts	SAVI
WBC [cells/µl] (age;reference range)	8600 (4300-10300)
ALC [cells/µl] (range: 1000-2800)	2236 1300-3500
B cells [cells/µl] (age;reference range)	1118 (200-1600)
T cells [cells/µl] (age;reference range)	1050 (700-4200)
CD4+ T cells [cells/µl] (age;reference range)	469 (300-2000)
CD8+ T cells [cells/µl] (age;reference range)	626 (300-1800)
NK cells [cells/µl] (age;reference range)	**↓44** (90-900)
Neutrophils [cells/µl] (age;reference range)	5848 (2100-6100)

Supplementary Table 3. Serologic findings and acute phase reactants of Patients

Serologic findings and acute phase reactants	Artem1	Artem2	Artem3	Artem4	Artem5	Artem6	Artem7	Artem8	Artem9	Artem10
IgG [mg/dl] (age;reference range)	**↓ 135** (3y; 640-2010)	**↓ 240** (3y; 640-2010)	1040 (8y; 764-2134)	**↓ 363** (5y; 745-1804)	1110 (8y;764-2134)	1190 (18y; 913-1884)	**↓ 560** (4y; 640-2010)	1140 (7y; 764-2134)	740 (3y; 640-2010)	**↓ 240** (5y; 745-1804)
IgG Subclasses [mg/dl] (age)	**IgG1=↓78,5, IgG2=↓ 51,5**	ne	**IgG1=599, IgG2=144, IgG3=62,6, IgG4=7,4** (8y)	**IgG1=↓289, IgG2=↓ 36, IgG3=17, IgG4=↓ 7** (5y)	ne	ne	**(IgG1=493, IgG2=↓70.4, IgG3=98.3, IgG4=↓ 7.7 (**4y)	**IgG1=844, IgG2=175, IgG3=67.5, IgG4=7.4** (7y)	ne	ne
IgM [mg/dl] (age;reference range)	**↓ 15** (3y; 52-297)	**↓ 35** (3y; 71-335)	**↓ 20.9** (8y; 69-387)	149 (5y; 78-261)	97 (8y; 69-387)	**↓ 86.9** (18y; 88-322)	54 (4y; 52-297)	86.5 (7y; 69-387)	410 (3y; 52-297)	**↓ 12** (5y; 78-261)
IgA [mg/dl] (age;reference range)	**↓ 6.6** (3y; 44-244)	**↓ 6.6** (3y6m; 26-296)	**↓ 24** (8y; 70-303)	**↓ 32.6** (5y; 57-282)	**↓ 6.6** (8y9m; 70-303)	**↓ 4.5** (18y; 139-378)	**↓ 18** (4y; 44-244)	**↓ 6.6** (7y; 70-303)	**↓ 6.6** (3y; 44-244)	**↓ 6.6** (5y; 57-282)
IgE [IU/ml] (age)	5	5	16.5	17	17.6	5	5	5	5	5
Vaccination response to Tetanus	0.11 (neg)	ne	0.98 (neg)	ne	ne	ne	ne	ne	0.04 (neg)	0.08 (neg)
Anti Hepatitis B surface antigen [mIU/ml]	0.51 (neg)	0.58 (neg)	1.35 (neg)	0 (neg)	ne	0.16 (neg)	3.5 (neg)	0 (neg)	0.4(neg)	33 (poz)
ESR (mm/h) (0-20y; 3-13)	3	5	7	**↑ 20**	4	7	2	2	**↑ 55**	3
CRP (mg/L) (<3)	**↑ 15.4**	<2	<2	**↑ 3.4**	**↑ 12.5**	1.9	<0.2	**↑ 7**	**↑ 90**	<2

ne: not examined

Serologic findings and acute phase reactants	AT1	AT2	AT3	AT4	AT5	AT6	AT7	AT8	AT9	AT10
IgG [mg/dl] (age;reference range)	1100 (745-1804)	1580 (745-1804)	1410 (640-2010)	↓170 (605-1430)	↓57 (304-1231)	849 (745-1804)	1280 (640-2010)	↓155 (604-1941)	↓534 (640-2010)	627 (604-1941)
IgG Subclasses [mg/dl] (age)	ne	ne	ne	ne	ne	ne	IgG1:1170 IgG2: 147 IgG3: 32 IgG4: 57	IgG1: 89 IgG2:33 IgG3: 50 IgG4:6	IgG1:568 IgG2:78 IgG3:10,5 IgG4:6,3	IgG1:345 IgG2:51 IgG3:20 IgG4:7
IgM [mg/dl] (age;reference range)	258 (78-261)	145 (78-261)	348 (52-297)	↑782 (66-228)	132 (32-203)	164 (78-261)	173 (52-297)	↑298 (71-235)	↓44 (52-297)	104 (71-235)
IgA [mg/dl] (age;reference range)	**↓<6.67** (57-282)	**↓<6.67** (57-282)	**↓<6.67** (14-544)	75 (30-107)	↓<6,6 (7-123)	↓<6.6 (57-232)	↓<6.6 (44-244)	115 (26-296)	↓24 (44-244)	↓<6,6 (26-296)
IgE [IU/ml] (age)	<1	<1	-	14	5	19	5	14	16	5
Vaccination response to Tetanus	ne	ne	ne	ne	ne	ne	ne	ne	ne	219
Anti Hepatitis B surface antigen [mIU/ml]	ne	ne	ne	1.7 (neg)	24 (poz)	ne	17	ne	ne	7.35
ESR (mm/h) (0-20y; 3-13)	**↑21**	12	**↑24**	**↑17**	**↑20**	5	9	**↑82**	11	1
CRP (mg/L) (<3)	0.419	0.658	0.6	<2	**↑6.6**	**↑12.5**	**↑5.5**	**↑3.6**	**↑16**	<2
AFP (0-40 ng/ml)				**↑73**	**↑116**	**↑188**	**↑43**	**↑86**	**↑60**	38

ne: not examined

Serologic findings and acute phase reactants	SAVI
IgG [mg/dl] (age;reference range)	↑ **5510** mg/dl (835-2094)
IgG Subclasses [mg/dl] (age)	ne
IgM [mg/dl] (age;reference range)	83 mg/dl (47-484)
IgA [mg/dl] (age;reference range)	394 mg/dl (67-433)
IgE [IU/ml] (age)	↑ **113** IU/ml (0-87)
Vaccination response to Tetanus	ne
Anti Hepatitis B surface antigen [mIU/ml]	20 (poz)
ESR (mm/h)	↑ **85**
CRP (mg/L)	0.6 (0.0-0.5)

ne: not examined